Generators BCVEGPY and GENXICC for doubly heavy mesons and baryons

Xing-Gang Wu

In collaboration with Profs.C.H.Chang, J.X.Wang, X.Y.Wang

Department of Physics, Chongquing University

16-21 May, ACAT 2013 at IHEP, P.R. China

Developed in about ten years

Generators for Bc meson and Xicc baryon events

1) << BCVEGPY1.0 …>> Comput.Phys.Commun.159, 192 (2004) – S-wave
2) << BCVEGPY2.0… >> Comput.Phys.Commun.174, 241 (2006) –P-wave
3) << BCVEGPY2.1 …>> Comput.Phys.Commun.175, 624(2006) – Linux
4) <<BCVEGPY2.2…>> Comput.Phys.Commun. 183,442 (2012) - Present version

==== BCVEGPY ↑ ======= GENXICC ↓ ====

5) << GENXICC1.0 …>> Comput.Phys.Commun.177, 467 (2007)
6) << GENXICC2.0 …>> Comput.Phys.Commun.181, 1144 (2010)
7) <<GENXICC2.1 …>> Comput.Phys.Commun. 184 , 1070(2013) - Present version

Directly related works for hadronic production of Bc meson and baryons

1) <<Uncertainties In Estimating Hadronic Production Of The Meson Bc and Comparisons Between Tevatron And Lhc>> Eur.Phys.J.C38, 267 (2004)

2) <<Hadronic Production Of The P-wave Excited Bc-states B*cJ, L=1 >> Phys.Rev.D 70, 114013 (2004)

3) << The Color-octet Contributions To P-wave Bc Meson Hadroproduction >> Phys.Rev.D 70, 074012 (2005)

4) << Hadronic Production Of Bc Meson Induced By The Heavy Quarks Inside The Collision Hadrons >> Phys.Rev.D 72, 114009 (2005)

5)<<Estimate of the hadronic production of the doubly charmed baryon Ξcc under GM-VFN scheme >>Phys.Rev. D34,094022 (2006)

6) << Hadronic production of the doubly charmed baryon Ξcc with intrinsic charm>> J.Phys. G34, 845 (2007)

7) << Hadronic Production of the Doubly Heavy Baryon Ξbc at LHC>> Phys.Rev. D83, 034026 (2011)

To agree with the purpose of the present conference, the main purpose of the present talk is to provide a detailed introduction to the

Improved Helicity Amplitude Technologies

To improve the efficiency of the generators

- Mechanisms for the Bc hadronic production

A) gluon-gluon fusion -------- dominant (our main concern)

color-singlet: S-wave: Bc (1), Bc*(~2.6); P-wave: Bc*(~ 0.5)

color-octet: S-wave: Bc+Bc* (~0.1)

B) quark-antiquark annihilation -----must be light quark

color-singlet: S-wave: Bc+Bc* (~0.1)

There are also extrinsic and intrinsic heavy quark mechanisms, in the generators, we do not consider them so far, which provide contributions in lower pt regions.

QCD factorization picture

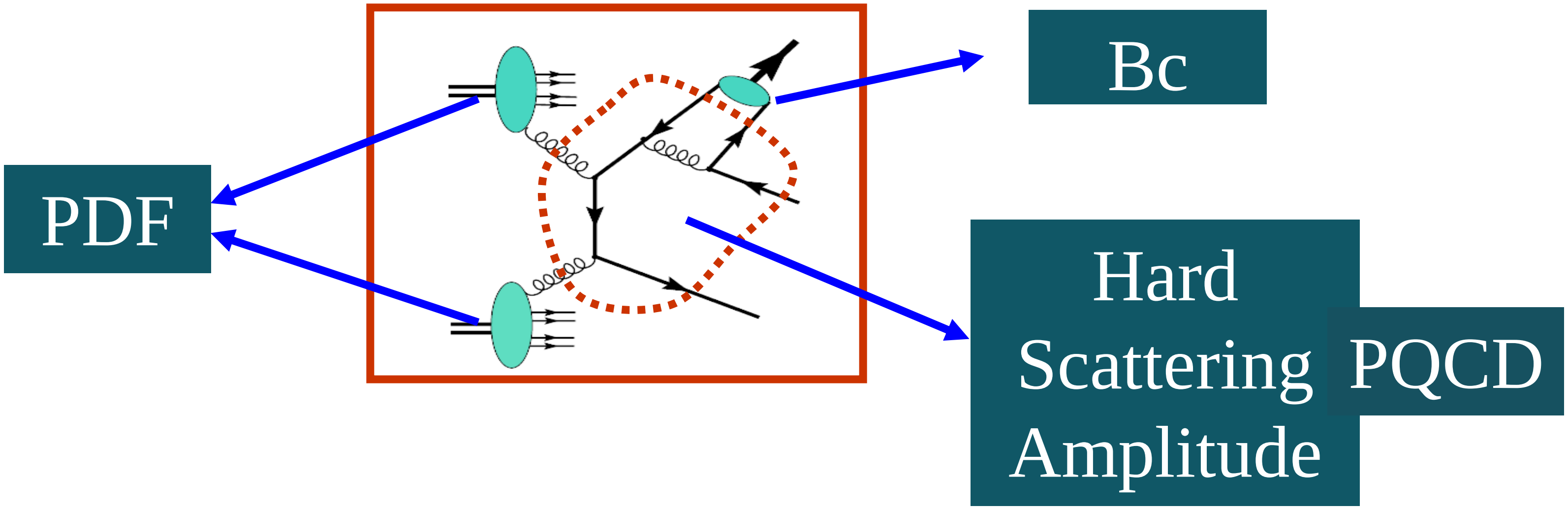

Differential cross-section for subprocess

$$d\hat{\sigma} = \frac{1}{2^{11}\times 3}\frac{(2\pi)^4|M|^2}{4(k_1\cdot k_2)} \times d\Phi_3(k_1+k_2;P,q_{b1},q_{c2}),$$

Three-body phase-space

RAMBOS → VEGAS

$$d\Phi_3(k_1+k_2;P,q_{b1},q_{c2}) = \delta^4(k_1+k_2-P-q_{b1}-q_{c2})\frac{d^3\vec{\mathbf{P}}}{(2\pi)^3 2E_P}\frac{d^3\vec{\mathbf{q}}_{b1}}{(2\pi)^3 2E_{q_{b1}}}\frac{d^3\vec{\mathbf{q}}_{c2}}{(2\pi)^3 2E_{q_{c2}}}.$$

Xicc similar to Bc case
Model: Diquark => Baryon

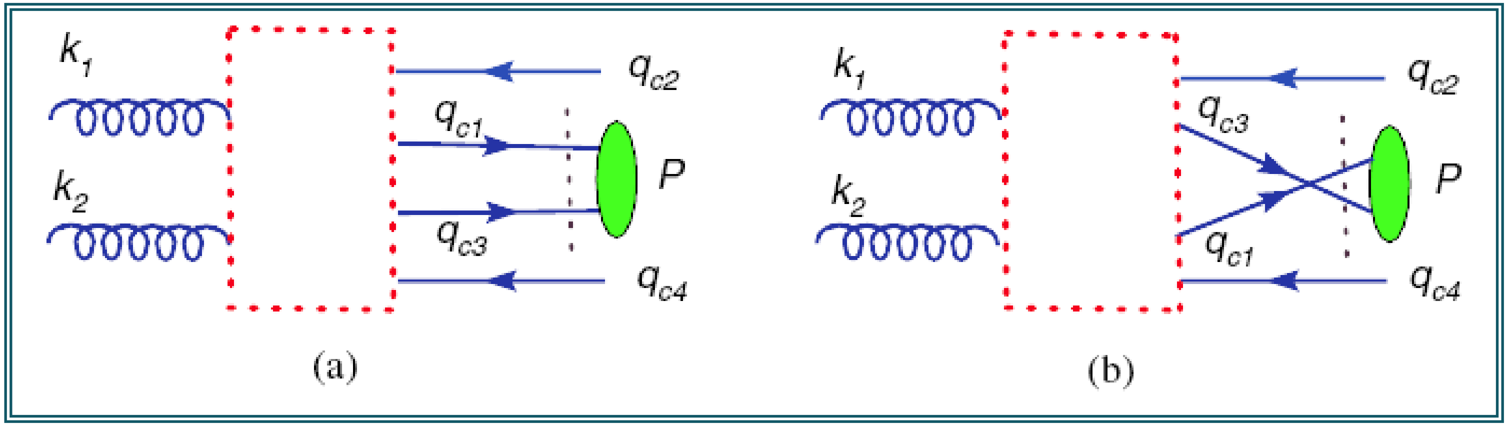

Quark lines

$$\mathrm{HME}_i = \langle q_{0\lambda_2}|(\not{q}_{c4} + m_c)\hat{\Gamma}_i(\not{q}_{c3} - m_c)|q_{0\lambda_1}\rangle,$$

$$\mathrm{HME}_i = -\langle q_{0(-\lambda_1)}|(\not{q}_{c3} + m_c)\Gamma_i(\not{q}_{c4} - m_c)|q_{0(-\lambda_2)}\rangle.$$

$$\langle p_{(\lambda_1)}|\not{k}_1 \dots \not{k}_n|q_{(\lambda_2)}\rangle = (-1)^{n+1}\langle q_{(-\lambda_2)}|\not{k}_n \dots \not{k}_1|p_{(-\lambda_1)}\rangle,$$

Color factor

TABLE V. The square of the six independent color factors (including the cross terms) for $gg \to (cc)_{\bar{3}}[^3S_1] + \bar{c} + \bar{c}$, $(C_{mij} \times C^*_{nij})$ with $m, n = (1, 2, \cdots, 6)$, respectively.

	C^*_{1ij}	C^*_{2ij}	C^*_{3ij}	C^*_{4ij}	C^*_{5ij}	C^*_{6ij}
C_{1ij}	$\frac{4}{3}$	$-\frac{1}{6}$	$\frac{2}{3}$	$-\frac{1}{12}$	$\frac{5}{12}$	$-\frac{1}{3}$
C_{2ij}	$-\frac{1}{6}$	$\frac{4}{3}$	$-\frac{1}{12}$	$\frac{2}{3}$	$-\frac{1}{3}$	$\frac{5}{12}$
C_{3ij}	$\frac{2}{3}$	$-\frac{1}{12}$	$\frac{4}{3}$	$-\frac{5}{12}$	$\frac{1}{12}$	$-\frac{2}{3}$
C_{4ij}	$-\frac{1}{12}$	$\frac{2}{3}$	$-\frac{5}{12}$	$\frac{4}{3}$	$-\frac{2}{3}$	$\frac{1}{12}$
C_{5ij}	$\frac{5}{12}$	$-\frac{1}{3}$	$\frac{1}{12}$	$-\frac{2}{3}$	$\frac{4}{3}$	$-\frac{1}{6}$
C_{6ij}	$-\frac{1}{3}$	$\frac{5}{12}$	$-\frac{2}{3}$	$\frac{1}{12}$	$-\frac{1}{6}$	$\frac{4}{3}$

TABLE VI. The square of the six independent color factors (including the cross terms) for $gg \to (cc)_{6}[^1S_0] + \bar{c} + \bar{c}$, $(C_{mij} \times C^*_{nij})$ with $m, n = (1, 2, \cdots, 6)$, respectively.

	C^*_{1ij}	C^*_{2ij}	C^*_{3ij}	C^*_{4ij}	C^*_{5ij}	C^*_{6ij}
C_{1ij}	$\frac{8}{3}$	$-\frac{1}{3}$	$\frac{2}{3}$	$-\frac{1}{12}$	$\frac{11}{12}$	$\frac{1}{6}$
C_{2ij}	$-\frac{1}{3}$	$\frac{8}{3}$	$-\frac{1}{12}$	$\frac{2}{3}$	$\frac{1}{6}$	$\frac{11}{12}$
C_{3ij}	$\frac{2}{3}$	$-\frac{1}{12}$	$\frac{8}{3}$	$\frac{11}{12}$	$-\frac{1}{12}$	$\frac{2}{3}$
C_{4ij}	$-\frac{1}{12}$	$\frac{2}{3}$	$\frac{11}{12}$	$\frac{8}{3}$	$\frac{2}{3}$	$-\frac{1}{12}$
C_{5ij}	$\frac{11}{12}$	$\frac{1}{6}$	$-\frac{1}{12}$	$\frac{2}{3}$	$\frac{8}{3}$	$-\frac{1}{3}$
C_{6ij}	$\frac{1}{6}$	$\frac{11}{12}$	$\frac{2}{3}$	$-\frac{1}{12}$	$-\frac{1}{3}$	$\frac{8}{3}$

BCVEGPY / GENXICC

gluon-gluon fusion

1) Helicity amplitude approach

To get the numerical value at the amplitude level

2) Detailed processes for the approach

Z. Xu, D.-H. Zhang, L. Chang, Nucl. Phys. B 291 (1987) 392.

quark

$$u_s(r) = \frac{1}{\sqrt{2r\cdot q}}(\not{r}+m)|q_h\rangle$$

$$v_s(r) = \frac{1}{\sqrt{2r\cdot q}}(\not{r}-m)|q_{-h}\rangle$$

gluon

$$\not{\epsilon}^{\pm}(k,q) = \frac{\sqrt{2}}{\langle q_{\mp}|k_{\pm}\rangle}\left[|k_{\mp}\rangle\langle q_{\mp}| + |q_{\pm}\rangle\langle k_{\pm}|\right]$$

$$\epsilon^{\pm}_{\mu}(k,q) = \langle k_{\pm}|\gamma_{\mu}|q_{\pm}\rangle/\sqrt{2}\langle q_{\mp}|k_{\pm}\rangle$$

Implying two ways of checking

The amplitude independent of the reference light-like momentum

Replacing the gluon polarization to its momentum, the amplitude must be zero

$$\gamma^0 = \begin{pmatrix} 0 & 1 \\ 1 & 0 \end{pmatrix}, \ \gamma^i = \begin{pmatrix} 0 & -\sigma^i \\ \sigma^i & 0 \end{pmatrix}, \ (i = 1, 2, 3)$$

$$\sigma^1 = \begin{pmatrix} 0 & 1 \\ 1 & 0 \end{pmatrix}, \ \sigma^2 = \begin{pmatrix} 0 & -i \\ i & 0 \end{pmatrix}, \ \sigma^3 = \begin{pmatrix} 1 & 0 \\ 0 & -1 \end{pmatrix},$$

$$k_\pm = k_0 \pm k_z, \ k_\perp = k_x + ik_y = |k_\perp| e^{i\varphi_k} = \sqrt{k_+ k_-} e^{i\varphi_k},$$

inner product

$$\langle k_1 \cdot k_2 \rangle = \langle k_{1-} | k_{2+} \rangle = \sqrt{k_{1-} k_{2+}} e^{i\varphi_1} - \sqrt{k_{1+} k_{2-}} e^{i\varphi_2}$$
$$= k_{1\perp} \sqrt{\frac{k_{2+}}{k_{1+}}} - k_{2\perp} \sqrt{\frac{k_{1+}}{k_{2+}}},$$

spinor product

Basic units

$$\langle k_{1+} | \not{k}_3 | k_{2+} \rangle = \langle k_{1+} | k_{3-} \rangle \langle k_{3-} | k_{2+} \rangle$$
$$= \frac{1}{\sqrt{k_{1+} k_{2+}}} (k_{1+} k_{2+} k_{3-} - k_{1+} k_{2\perp} k_{3\perp}^* - k_{1\perp}^* k_{2+} k_{3\perp} + k_{1\perp}^* k_{2\perp} k_{3+})$$

$$P' = P - \frac{P^2}{2P \cdot q_0} q_0.$$

$$\langle q_{0+} | \not{\epsilon}(s_z) \not{P}' | q_{0-} \rangle = P'_+ \epsilon(s_z)_- q_{0\perp}^* - (P'_\perp)^* q_{0+} \epsilon(s_z)_- - P'_+ \epsilon(s_z)_\perp \frac{q_{0\perp}^{*2}}{q_{0+}} + \epsilon(s_z)_\perp (P'_\perp)^* q_{0\perp}^*$$
$$- P'_\perp \epsilon(s_z)_\perp^* q_{0\perp}^* + q_{0+} \epsilon_\perp^* P'_- + \epsilon(s_z)_+ P'_\perp \frac{q_{0\perp}^{*2}}{q_{0+}} - \epsilon(s_z)_+ P'_- q_{0\perp}^*$$

Diagrammatically or schematically

Decompose the diagram

Find out all the independent fermion lines “bases”

Simplify the fermion lines “bases”

Expande all the Feynman amplitude over these bases and find out the corresponding coefficients

Numerical calculation

Great improvement ! for massless lines

Divide the whole amplitude into several gauge invariant groups, and simplify each group with proper gauges.

Problem/complexity： 1： how to choose gauge in each group； 2： stability of numerical calculation； 3： no help for the massive fermion lines.

$$\not\epsilon^{\pm}(k,q) = \frac{\sqrt{2}}{\langle q_{\mp}|k_{\pm}\rangle}\left[|k_{\mp}\rangle\langle q_{\mp}| + |q_{\pm}\rangle\langle k_{\pm}|\right]$$

$$\epsilon^{\pm}_{\mu}(k,q) = \langle k_{\pm}|\gamma_{\mu}|q_{\pm}\rangle/\sqrt{2}\langle q_{\mp}|k_{\pm}\rangle$$

Our method

$$g + g \to c + \bar{b} + b + \bar{c}$$

substruction

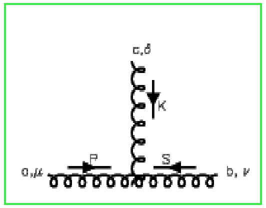

$$\frac{1}{P^2Q^2} = \frac{1}{P^2(Q^2-P^2)} + \frac{1}{Q^2(P^2-Q^2)},$$

$$\frac{1}{P^2Q^2R^2} = \frac{1}{P^2(Q^2-P^2)(R^2-P^2)} + \frac{1}{Q^2(P^2-Q^2)(R^2-Q^2)} + \frac{1}{R^2(P^2-R^2)(Q^2-R^2)} \quad (47)$$

man-made singularity

Corrected Feynman rule needed for decomposing:

Temporary extra terms

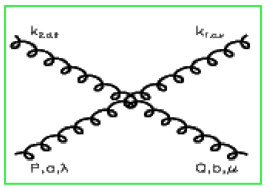

$$g f_{abc} \tilde{T}^{\mu\nu\delta}(P,S,K) = g f_{abc} T^{\mu\nu\delta}(P,S,K) + g f_{abc} G^{\mu\nu\delta}(P,S,K),$$

$$-ig\tilde{V}^{\lambda\mu\nu\delta}_{abcd}(P,Q,K_1,k_2) = -igV^{\lambda\mu\nu\delta}_{abcd}(P,Q,K_1,k_2) - igG^{\lambda\mu\nu\delta}_{abcd}(P,Q,K_1,k_2),$$

Used for demonstration of gauge invariance

where $T^{\mu\nu\delta}(P,S,K)$ and $V^{\lambda\mu\nu\delta}_{abcd}(P,Q,K_1,k_2)$ are the primary Feynman rules

$$T^{\mu\nu\delta}(P,S,K) = (P-S)^\delta g^{\mu\nu} + (S-K)^\mu g^{\delta\nu} + (K-P)^\nu g^{\delta\mu}$$

$$V^{\lambda\mu\nu\delta}_{abcd}(P,Q,K_1,k_2) = f_{abe}f_{cde}(g^{\lambda\nu}g^{\mu\delta} - g^{\lambda\delta}g^{\mu\nu}) + f_{ace}f_{dbe}(g^{\lambda\delta}g^{\mu\nu} - g^{\lambda\mu}g^{\nu\delta}) + f_{ade}f_{bce}(g^{\lambda\mu}g^{\nu\delta} - g^{\lambda\nu}g^{\mu\delta}),$$

and $G^{\mu\nu\delta}(P,S,K)$ and $G^{\lambda\mu\nu\delta}_{abcd}(P,Q,K_1,k_2)$ are the modified part

$$G^{\mu\nu\delta}(P,S,K) = (\pm)(P^\mu P^\nu P^\delta/(P\cdot K) + S^\mu S^\nu S^\delta/(S\cdot K))$$

$$G^{\lambda\mu\nu\delta}_{abcd}(P,Q,K_1,k_2) = -f_{ace}f_{bde}\frac{S_1^\lambda S_1^\mu S_1^\nu S_1^\delta}{(S_1\cdot K_1)(S_1\cdot K_2)} - f_{ade}f_{bce}\frac{S_2^\lambda S_2^\mu S_2^\nu S_2^\delta}{(S_2\cdot K_1)(S_2\cdot K_2)},$$

Replacing the polarization vector by the gluon momentum

APPENDIX A: GAUGE INVARIANCE OF THE cb SUBSET

Totally there are four gauge invariant subset cc, bb, cb, bc, we list here the demonstration of the gauge invariance of the cb and the cc subsets ,while the gauge invariance of the other two subsets can be easily demonstrated by the gluon symmetry.

The involved matrix elements are $M_{cb1}, M_{cb2}, M_{cb3}, M_{cb4}, M_{ca1}, M_{ca2}, M_{ob1}, M_{ob2}, M_{oa2}$. To demonstrate the gauge invariance we set $\not\epsilon_1^{\lambda_1} = \not k_1$ and $\not\epsilon_2^{\lambda_2} = \not k_2$, then we obtain for the primary matrix elements:

$$M_{cb1} = (-C_{1ij})\bar{u}_b\gamma_\alpha\psi_P\gamma_\alpha v_c \cdot \frac{1}{s_2}, \quad \text{(A1)}$$

$$M_{cb2} = (C_{3ij})\bar{u}_b\gamma_\alpha\psi_P\gamma_\alpha v_c \cdot \frac{1}{s_2}, \quad \text{(A2)}$$

$$\frac{1}{(s_c - s_b)(s_1 - s_b)} + \frac{1}{(s_b - s_1)(s_c - s_1)} + \frac{1}{(s_b - s_c)(s_1 - s_c)} = 0$$

$$M_{cb3} = (C_{3ij})\bar{u}_b\gamma_\alpha\psi_P\gamma_\alpha v_c \cdot \frac{1}{s_2}, \quad \text{(A3)}$$

$$M_{cb4} = (C_{5ij} - C_{3ij})\bar{u}_b\gamma_\alpha\psi_P\gamma_\alpha v_c \cdot \frac{1}{s_2}, \quad \text{(A4)}$$

$$(M_{ca1})_{cb} = (c_{3ij} - C_{1ij})\left(-\bar{u}_b\gamma_\alpha\psi_P\gamma_\alpha v_c \cdot \frac{1}{s_2} + \bar{u}_b\not k_2\psi_P\not k_1 v_c \cdot \frac{1}{s_2(s_b - s_2)}\right), \quad \text{(A5)}$$

$$(M_{ca2})_{cb} = (-C_{5ij})\left(\bar{u}_b\gamma_\alpha\psi_P\gamma_\alpha v_c \cdot \frac{1}{s_2} - \bar{u}_b\not k_2\psi_P\not k_1 v_c \cdot \frac{1}{s_2(s_b - s_2)}\right), \quad \text{(A6)}$$

$$(M_{ob1})_{cb} = (C_{3ij} - C_{1ij})\left(-\bar{u}_b\gamma_\alpha\psi_P\gamma_\alpha v_c \cdot \frac{1}{s_2} + \bar{u}_b\not k_2\psi_P\not k_1 v_c \cdot \frac{1}{s_2(s_c - s_2)}\right), \quad \text{(A7)}$$

$$(M_{ob2})_{cb} = (-C_{5ij})\left(\bar{u}_b\gamma_\alpha\psi_P\gamma_\alpha v_c \cdot \frac{1}{s_2} - \bar{u}_b\not k_2\psi_P\not k_1 v_c \cdot \frac{1}{s_2(s_c - s_2)}\right), \quad \text{(A8)}$$

$$(M_{oa2})_{cb} = (C_{1ij} - C_{3ij} - C_{5ij})\left(-\bar{u}_b\gamma_\alpha\psi_P\gamma_\alpha v_c \cdot \frac{1}{s_2} + \bar{u}_b\not k_2\psi_P\not k_1 v_c \cdot \frac{s_c + s_b - s_2}{s_2(s_b - s_2)(s_c - s_2)}\right), \quad \text{(A9)}$$

where i, j are the quark's color indexes and $(M_{oa2})_{cb}$ is the part of M_{oa2} that attributes to the cb subset, and so on.

While for the matrix elements containing the modified part, by carefully fixed the sign of the modified part of 3-gluon vertex, we obtain

$$(M^c_{ca1})_{cb} + (M^c_{ca2})_{cb} = (C_{1ij} - C_{3ij} - C_{5ij})\bar{u}_b\not k_2\psi_P\not k_1 v_c \cdot \frac{1}{s_2(s_b - s_2)}, \quad \text{(A10)}$$

$$(M^c_{ob1})_{cb} + (M^c_{ob2})_{cb} = (C_{1ij} - C_{3ij} - C_{5ij})\bar{u}_b\not k_2\psi_P\not k_1 v_c \cdot \frac{1}{s_2(s_c - s_2)}, \quad \text{(A11)}$$

$$(M^c_{oa2})_{cb} = (C_{1ij} - C_{3ij} - C_{5ij})\bar{u}_b\not k_2\psi_P\not k_1 v_c \cdot \frac{s_2 - s_c - s_b}{s_2(s_b - s_2)(s_c - s_2)}. \quad \text{(A12)}$$

When add all these terms together, we get the desired result that all of them are cancelled out exactly.

Replacing the polarization vector by the gluon momentum

APPENDIX B: GAUGE INVARIANCE OF THE cc SUBSET

For the cc subset, the involved matrix elements are M_{cc1}, M_{cc2} ,..., M_{cc8}, M_{oc1} , M_{oc2}, M_{co1} ,M_{co2} , M_{oo1}, M_{oo2} , M_{oo3}, M_{oo4}. To demonstrate the gauge invariance we also set $\not{\epsilon}_1^{\lambda_1} = \not{k}_1$ and $\not{\epsilon}_2^{\lambda_2} = \not{k}_2$, then we obtain for the primary matrix elements:

$$M_{cc1} + M_{cc2} + M_{cc7} = (C_{1ij} + C_{2ij})\bar{u}_b\gamma_\delta\psi_P\gamma_\delta v_c\frac{1}{2s_b}, \quad \text{(B1)}$$

$$M_{cc3} = (-C_{4ij})\bar{u}_b\gamma_\delta\psi_P\gamma_\delta v_c\frac{1}{s_b}, \quad \text{(B2)}$$

$$M_{cc4} = (-C_{3ij})\bar{u}_b\gamma_\delta\psi_P\gamma_\delta v_c\frac{1}{s_b}, \quad \text{(B3)}$$

$$M_{cc5} + M_{cc6} + M_{cc8} = (C_{3ij} + C_{4ij} - 2C_{5ij})\bar{u}_b\gamma_\delta\psi_P\gamma_\delta v_c\frac{1}{2s_b}, \quad \text{(B4)}$$

$$(M_{oc1})_{cc} = (C_{4ij} - C_{2ij})\frac{1}{s_b(s_a - s_b)}(\bar{u}_b\not{k}_1\psi_P\not{k}_2 v_c + (s_1 - s_b)\bar{u}_b\gamma_\delta\psi_P\gamma_\delta v_c), \quad \text{(B5)}$$

$$(M_{co1})_{cc} = (C_{3ij} - C_{1ij})\frac{1}{s_b(s_a - s_b)}(\bar{u}_b\not{k}_2\psi_P\not{k}_1 v_c + (s_2 - s_b)\bar{u}_b\gamma_\delta\psi_P\gamma_\delta v_c), \quad \text{(B6)}$$

$$(M_{oc2})_{cc} = (C_{5ij})\frac{1}{s_b(s_a - s_b)}(\bar{u}_b\not{k}_1\psi_P\not{k}_2 v_c + (s_1 - s_b)\bar{u}_b\gamma_\delta\psi_P\gamma_\delta v_c), \quad \text{(B7)}$$

$$(M_{co2})_{cc} = (C_{5ij})\frac{1}{s_b(s_a - s_b)}(\bar{u}_b\not{k}_2\psi_P\not{k}_1 v_c + (s_2 - s_b)\bar{u}_b\gamma_\delta\psi_P\gamma_\delta v_c), \quad \text{(B8)}$$

$$(M_{oo1})_{cc} = (C_{2ij} - C_{4ij} - C_{5ij})\left(\frac{s_2 + s_k}{s_b(s_1 - s_b)(s_a - s_b)}(\bar{u}_b\not{k}_2\psi_P\not{k}_1 v_c) + \frac{s_a - s_1}{s_b(s_a - s_b)}\bar{u}_b\gamma_\delta\psi_P\gamma_\delta v_c\right) \quad \text{(B9)}$$

$$(M_{oo2})_{cc} = (C_{1ij} - C_{3ij} - C_{5ij})\left(\frac{s_1 + s_k}{s_b(s_2 - s_b)(s_a - s_b)}(\bar{u}_b\not{k}_1\psi_P\not{k}_2 v_c) + \frac{s_a - s_2}{s_b(s_a - s_b)}\bar{u}_b\gamma_\delta\psi_P\gamma_\delta v_c\right) \quad \text{(B10)}$$

$$(M_{oo3})_{cc} = (C_{1ij} + C_{4ij} - C_{2ij} - C_{3ij})\left(\frac{1}{s_b(s_a - s_b)}(2\bar{u}_b\not{k}_2\psi_P\not{k}_1 v_c - 2\bar{u}_b\not{k}_1\psi_P\not{k}_2 v_c) + \frac{s_2 - s_1}{2s_b(s_a - s_b)}\bar{u}_b\gamma_\delta\psi_P\gamma_\delta v_c\right), \quad \text{(B11)}$$

$$\frac{1}{(s_a - s_b)(s_1 - s_b)} + \frac{1}{(s_b - s_1)(s_a - s_1)} + \frac{1}{(s_b - s_a)(s_1 - s_a)} = 0$$

Replacing the polarization vector by the gluon momentum

$$(M_{oo4})_{oo} = \frac{1}{s_b(s_a-s_b)}\Big((2C_{2ij}-2C_{4ij}+C_{3ij}-C_{1ij}-C_{5ij})\bar{u}_b\not{k}_2\not{\epsilon}_P\not{k}_1 v_a + (2C_{1ij}-2C_{3ij}+C_{4ij} -C_{2ij}-C_{5ij})\bar{u}_b\not{k}_1\not{\epsilon}_P\not{k}_2 v_a + (C_{3ij}+C_{4ij}-C_{1ij}-C_{2ij}+2C_{5ij})\frac{s_k}{2}\bar{u}_b\gamma_\delta\not{\epsilon}_P\gamma_\delta v_a\Big). \quad \text{(B12)}$$

Adding all these terms together and by using the relation

$$s_b + s_a - s_1 - s_2 - s_k = 0,$$

we obtain

$$M_{oa1}+\ldots+M_{oa8}+(M_{oo1})_{oo}+\ldots+(M_{oo2})_{oo}+(M_{oo1})_{oo}+\ldots+(M_{oo4})_{oo} = (c_{4ij}-C_{2ij}+C_{5ij})\bar{u}_b\not{k}_1\not{\epsilon}_P\not{k}_2 v_a\frac{s_b-2s_a}{s_b(s_1-s_b)(s_a-s_b)} + (c_{3ij}-C_{1ij}+C_{5ij})\bar{u}_b\not{k}_2\not{\epsilon}_P\not{k}_1 v_a\frac{s_b-2s_a}{s_b(s_2-s_b)(s_a-s_b)} \quad \text{(B13)}$$

For the matrix elements involving the modified part, we have

$$M^a_{oa7}+M^a_{oa8} = C_{003}\frac{1}{2s_b}\bar{u}_b\gamma_\delta\not{\epsilon}_P\gamma_\delta v_a, \quad \text{(B14)}$$

$$(M^a_{oo3})_{oo} = -C_{003}\frac{1}{2s_b}\bar{u}_b\gamma_\delta\not{\epsilon}_P\gamma_\delta v_a, \quad \text{(B15)}$$

$$(M^a_{oo1}+M^a_{oa2})_{oo} = C_{001}\frac{1}{s_b(s_b-s_1)}\bar{u}_b\not{k}_1\not{\epsilon}_P\not{k}_2 v_a, \quad \text{(B16)}$$

$$(M^a_{oo2}+M^a_{oa1})_{oo} = C_{002}\frac{1}{s_b(s_b-s_2)}\bar{u}_b\not{k}_2\not{\epsilon}_P\not{k}_1 v_a, \quad \text{(B17)}$$

$$(M^a_{oo1})_{oo} = C_{001}\frac{s_1-s_b-s_a}{s_b(s_a-s_b)(s_1-s_b)}\bar{u}_b\not{k}_1\not{\epsilon}_P\not{k}_2 v_a, \quad \text{(B18)}$$

$$(M^a_{oo2})_{oo} = C_{002}\frac{s_2-s_b-s_a}{s_b(s_a-s_b)(s_2-s_b)}\bar{u}_b\not{k}_2\not{\epsilon}_P\not{k}_1 v_a, \quad \text{(B19)}$$

$$(M^a_{oo4})_{oo} = -C_{002}\frac{1}{s_b(s_a-s_b)}\bar{u}_b\not{k}_2\not{\epsilon}_P\not{k}_1 v_a - C_{001}\frac{1}{s_b(s_a-s_b)}\bar{u}_b\not{k}_1\not{\epsilon}_P\not{k}_2 v_a. \quad \text{(B20)}$$

where the color factors

$$C_{001} = C_{2ij}-C_{4ij}-C_{5ij},$$
$$C_{002} = C_{1ij}-C_{3ij}-C_{5ij},$$
$$C_{003} = C_{1ij}+C_{4ij}-C_{2ij}-C_{3ij}. \quad \text{(B21)}$$

When adding all these modified terms together we obtain

$$M^a_{oa7}+M^a_{oa8}+(M^a_{oo1})_{oo}+\ldots+(M^a_{oa2})_{oo}+(M^a_{oa1})_{oo}+\ldots+(M^a_{oo4})_{oo} = (c_{4ij}-C_{2ij}+C_{5ij})\bar{u}_b\not{k}_1\not{\epsilon}_P\not{k}_2 v_a\frac{2s_a-s_b}{s_b(s_1-s_b)(s_a-s_b)} + (c_{3ij}-C_{1ij}+C_{5ij})\bar{u}_b\not{k}_2\not{\epsilon}_P\not{k}_1 v_a\frac{2s_a-s_b}{s_b(s_2-s_b)(s_a-s_b)} \quad \text{(B22)}$$

Adding Eq.(B13) and Eq.(B22) together, we get the desired result.

polarization vector

$$
\begin{aligned}
M^c_{total} = & \Bigg[\bar{u}_b \not{k}_1 \psi_P \not{k}_2 v_c \left(\frac{(q_{c+}+q_{c-})\cdot\epsilon_{2c}^{\lambda_2}}{(q_{c+}+q_{c-})\cdot k_2} \cdot \frac{(q_{b+}+q_{b-})\cdot\epsilon_{1c}^{\lambda_1}}{(q_{b+}+q_{b-})\cdot k_1} \right) - \bar{u}_b \not{k}_1 \psi_P \not{\epsilon}_{2c}^{\lambda_2} v_c \left(\frac{2(q_{b+}+q_{b-})\cdot\epsilon_{1c}^{\lambda_1}}{(s_b-s_1)} \right) \\
& -\bar{u}_b \not{\epsilon}_{1c}^{\lambda_1} \psi_P \not{k}_2 v_c \left(\frac{2(q_{c+}+q_{c-})\cdot\epsilon_{2c}^{\lambda_2}}{(s_c-s_1)} \right) \Bigg] \cdot \frac{C_{001}}{(s_c-s_b)(s_1-s_b)} + \\
& \Bigg[\bar{u}_b \not{k}_1 \psi_P \not{k}_2 v_c \left(\frac{(q_{c+}+q_{c-})\cdot\epsilon_{2c}^{\lambda_2}}{(q_{c+}+q_{c-})\cdot k_2} \cdot \frac{(q_{b+}+q_{b-})\cdot\epsilon_{1b}^{\lambda_1}}{(q_{b+}+q_{b-})\cdot k_1} \right) - \bar{u}_b \not{k}_1 \psi_P \not{\epsilon}_{2c}^{\lambda_2} v_c \left(\frac{2(q_{b+}+q_{b-})\cdot\epsilon_{1b}^{\lambda_1}}{(s_b-s_1)} \right) \\
& -\bar{u}_b \not{\epsilon}_{1b}^{\lambda_1} \psi_P \not{k}_2 v_c \left(\frac{2(q_{c+}+q_{c-})\cdot\epsilon_{2c}^{\lambda_2}}{(s_c-s_1)} \right) \Bigg] \cdot \frac{C_{001}}{(s_c-s_1)(s_b-s_1)} + \\
& \Bigg[\bar{u}_b \not{k}_1 \psi_P \not{k}_2 v_c \left(\frac{(q_{c+}+q_{c-})\cdot\epsilon_{2b}^{\lambda_2}}{(q_{c+}+q_{c-})\cdot k_2} \cdot \frac{(q_{b+}+q_{b-})\cdot\epsilon_{1b}^{\lambda_1}}{(q_{b+}+q_{b-})\cdot k_1} \right) - \bar{u}_b \not{k}_1 \psi_P \not{\epsilon}_{2b}^{\lambda_2} v_c \left(\frac{2(q_{b+}+q_{b-})\cdot\epsilon_{1b}^{\lambda_1}}{(s_b-s_1)} \right) \\
& -\bar{u}_b \not{\epsilon}_{1b}^{\lambda_1} \psi_P \not{k}_2 v_c \left(\frac{2(q_{c+}+q_{c-})\cdot\epsilon_{2b}^{\lambda_2}}{(s_c-s_1)} \right) \Bigg] \cdot \frac{C_{001}}{(s_b-s_c)(s_1-s_c)} + \\
& \Bigg[\bar{u}_b \not{k}_2 \psi_P \not{k}_1 v_c \left(\frac{(q_{c+}+q_{c-})\cdot\epsilon_{1c}^{\lambda_1}}{(q_{c+}+q_{c-})\cdot k_1} \cdot \frac{(q_{b+}+q_{b-})\cdot\epsilon_{2c}^{\lambda_2}}{(q_{b+}+q_{b-})\cdot k_2} \right) - \bar{u}_b \not{k}_2 \psi_P \not{\epsilon}_{1c}^{\lambda_1} v_c \left(\frac{2(q_{b+}+q_{b-})\cdot\epsilon_{2c}^{\lambda_2}}{(s_b-s_2)} \right) \\
& -\bar{u}_b \not{\epsilon}_{2c}^{\lambda_2} \psi_P \not{k}_1 v_c \left(\frac{2(q_{c+}+q_{c-})\cdot\epsilon_{1c}^{\lambda_1}}{(s_c-s_2)} \right) \Bigg] \cdot \frac{C_{002}}{(s_c-s_b)(s_2-s_b)} + \\
& \Bigg[\bar{u}_b \not{k}_2 \psi_P \not{k}_1 v_c \left(\frac{(q_{c+}+q_{c-})\cdot\epsilon_{1c}^{\lambda_1}}{(q_{c+}+q_{c-})\cdot k_1} \cdot \frac{(q_{b+}+q_{b-})\cdot\epsilon_{2b}^{\lambda_2}}{(q_{b+}+q_{b-})\cdot k_2} \right) - \bar{u}_b \not{k}_2 \psi_P \not{\epsilon}_{1c}^{\lambda_1} v_c \left(\frac{2(q_{b+}+q_{b-})\cdot\epsilon_{2b}^{\lambda_2}}{(s_b-s_2)} \right) \\
& -\bar{u}_b \not{\epsilon}_{2b}^{\lambda_2} \psi_P \not{k}_1 v_c \left(\frac{2(q_{c+}+q_{c-})\cdot\epsilon_{1c}^{\lambda_1}}{(s_c-s_2)} \right) \Bigg] \cdot \frac{C_{002}}{(s_c-s_2)(s_b-s_2)} + \\
& \Bigg[\bar{u}_b \not{k}_2 \psi_P \not{k}_1 v_c \left(\frac{(q_{c+}+q_{c-})\cdot\epsilon_{1b}^{\lambda_1}}{(q_{c+}+q_{c-})\cdot k_1} \cdot \frac{(q_{b+}+q_{b-})\cdot\epsilon_{2b}^{\lambda_2}}{(q_{b+}+q_{b-})\cdot k_2} \right) - \bar{u}_b \not{k}_2 \psi_P \not{\epsilon}_{1b}^{\lambda_1} v_c \left(\frac{2(q_{b+}+q_{b-})\cdot\epsilon_{2b}^{\lambda_2}}{(s_b-s_2)} \right) \\
& -\bar{u}_b \not{\epsilon}_{2b}^{\lambda_2} \psi_P \not{k}_1 v_c \left(\frac{2(q_{c+}+q_{c-})\cdot\epsilon_{1b}^{\lambda_1}}{(s_c-s_2)} \right) \Bigg] \cdot \frac{C_{002}}{(s_b-s_c)(s_2-s_c)}.
\end{aligned}
$$

Contributions from the extra terms can not equal to zero for the massive case !

BACK

All the quark mass tends to zero

$$\bar{u}_b \not{\epsilon}_b^{\lambda_i} v_b = \bar{u}_c \not{\epsilon}_c^{\lambda_i} v_c = 0,$$

$$M^c_{total} = 0.$$

$$gg \longrightarrow q\bar{q}q\bar{q}$$

$$u_s(r) = \frac{1}{\sqrt{2r\cdot q}}(\not{r}+m)|q_h\rangle \qquad \not{\epsilon}^{\pm}(k,q) = \frac{\sqrt{2}}{\langle q_{\mp}|k_{\pm}\rangle}[|k_{\mp}\rangle\langle q_{\mp}| + |q_{\pm}\rangle\langle k_{\pm}|]$$

$$v_s(r) = \frac{1}{\sqrt{2r\cdot q}}(\not{r}-m)|q_{-h}\rangle \qquad \epsilon^{\pm}_{\mu}(k,q) = \langle k_{\pm}|\gamma_\mu|q_{\pm}\rangle/\sqrt{2}\langle q_{\mp}|k_{\pm}\rangle$$

the massive fermions have time-like momenta q_i $(i=1,2)$ and $\not{q}_i$ are directly connected to $|q_{0\lambda_i}\rangle$ or $\langle q_{0\lambda_i}|$ as in Eq.(28), we may introduce the light-like momenta by defining

$$q_i' = q_i - \frac{q_i^2}{2q_i\cdot q_0}q_0\,.$$

$$\not{q}_i' = |q_i'+\rangle\langle q_i'+| + |q_i'-\rangle\langle q_i'-|$$

Then $\not{q}_i$ for massive fermions can be replaced by the massless ones, $\not{q}'_i$, without any consequences. This is due to the relations $\not{q}_0|q_{0\lambda_i}\rangle = 0$ or $\langle q_{0\lambda_i}|\not{q}_0 = 0\,.$

Step by step, change all the space-like momentua into light-like.

Fermion line

Basic QED-like diagram

Unified gauge: The arbitrary reference light-like momentum in the massive spinor, the polarization vector and in all the intermediate space-like momentum transformation can be taken to be the same. In this way the amplitude can be fully simplified.

Condensed results that are expressed by the **spinor inner product and spinor products.**

Key point: using the symmetries of the Feynman diagrams

Construct all the Feynman with all the independent QED-like Feynman diagrams, with the help of the quark-antiquark and gluon-gluon symmetries.

Unite the same type terms as much as possible

Complete the program based on the Feynman diagrams.

Most Effective Generator!

CALCULATIONS BASED on the diagram

3) More details of our approach

Helicity Amplitude Approach

A、basic idea, decomposition of the Feynman diagrams

How to Decompose 36 Feynmans ?
Skeleton QED-like

B、five groups of diagrams,

according to its topologies

Find nine basic Feynman diagrams

Find eight quark lines

Gluon-gluon and quark-quark exchange

Nine basic diagrams

Not unique

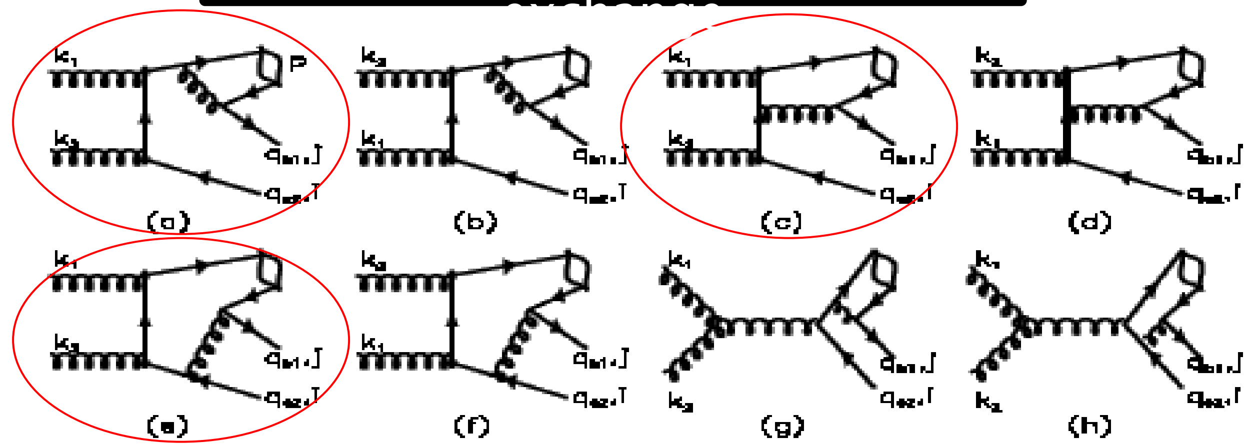

Feynman diagrams that can be directly grouped into the *cc* subset. Here *i* and *j*

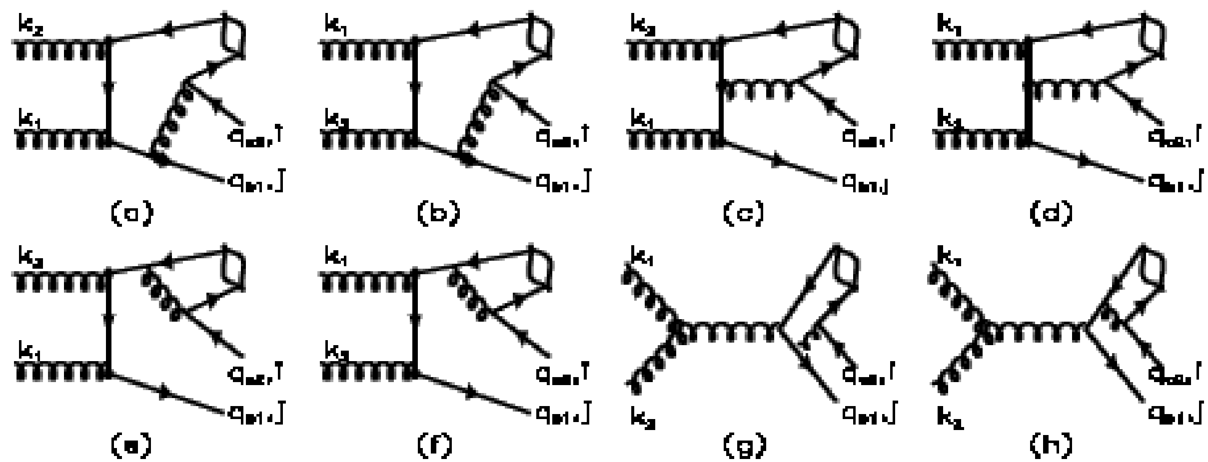

Feynman diagrams that can be directly grouped into the *bb* subset. Here *i* and *j*

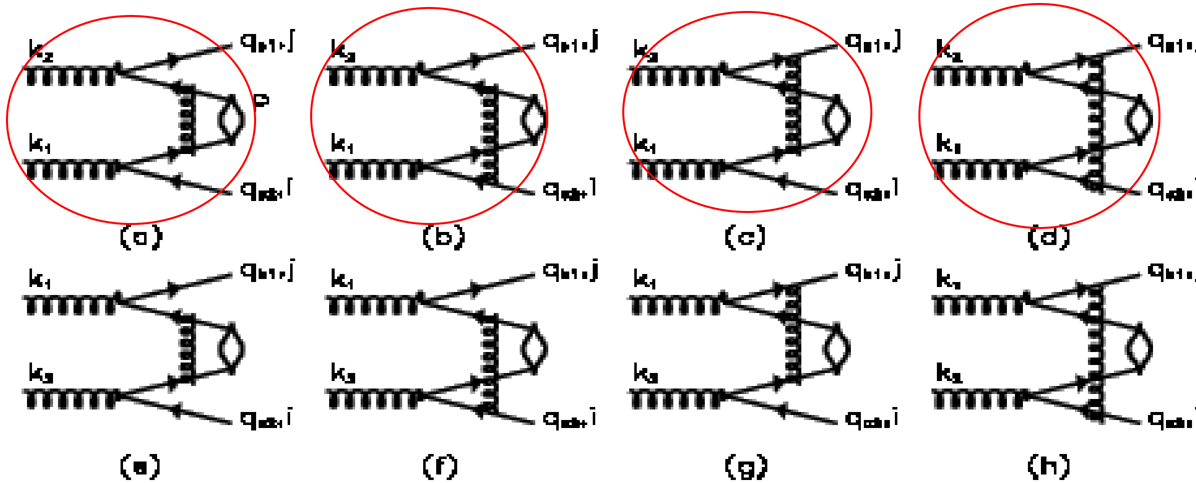

Feynman diagrams that can be directly grouped into the *cb* or *bc* subsets, where

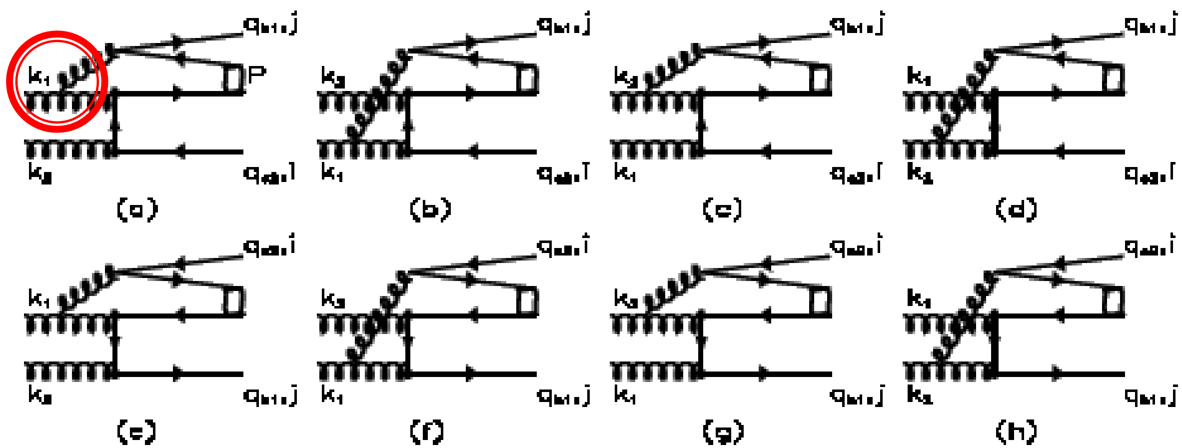

Decompose

Decompose

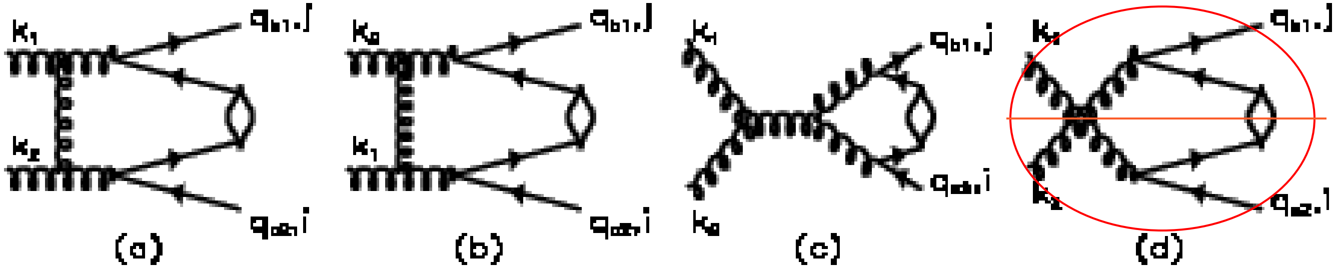

C、decompose the three gluon vertex

Basic

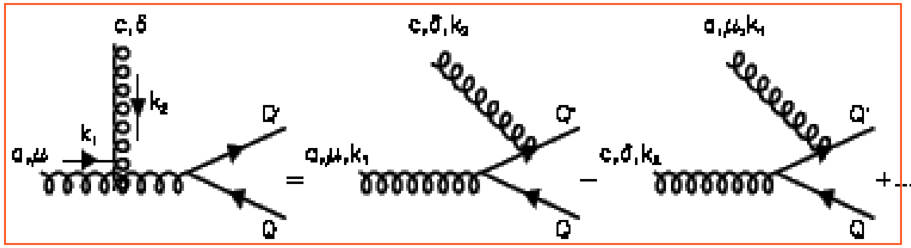

QCD-like → QED-like

FIG. 6: The three-gluon coupling vertex is decomposed as in Eq.(16): the first two terms are the 'basic QED-like' terms and the 'remaining' terms are expressed by several extra basic functions.

Cut off the color factor and the scalar part of the propagator

$$M^{ac}_{\delta\mu} \simeq \gamma_\delta(\not{k}_1 - \not{Q} + M)\gamma_\mu - \gamma_\mu(\not{k}_2 - \not{Q} + M)\gamma_\delta + (\not{Q}' - M)(\gamma_\delta\gamma_\mu - g_{\mu\delta})$$
$$+(\gamma_\mu\gamma_\delta - g_{\mu\delta})(\not{Q} + M) + k_{2\delta}\gamma_\mu - k_{1\mu}\gamma_\delta$$

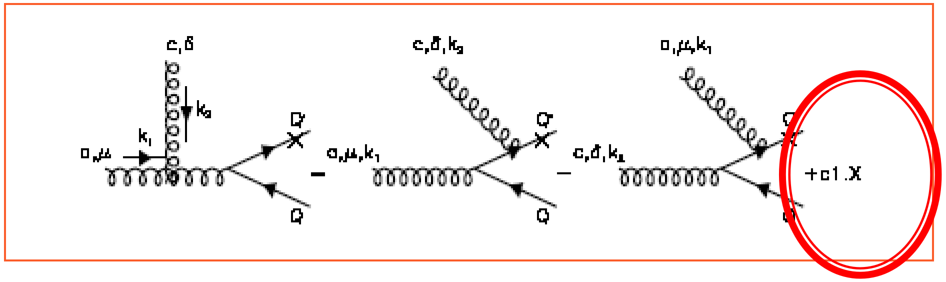

QCD-like → QED-like

$$M^{acd}_{\mu\delta\alpha}(k_1, k_2, Q, Q') \simeq \bar{u}(Q')\gamma_\alpha(\not{k}_1 + \not{k}_2 - \not{Q} + M)\Big(\gamma_\delta(\not{k}_1 - \not{Q} + M)\gamma_\mu -$$
$$\gamma_\mu(\not{k}_2 - \not{Q} + M)\gamma_\delta\Big)v(Q) + (C1 \cdot X) + \cdots$$

where

$$c1 = m_1^2 + m_2^2 + 2k_1 \cdot k_2 - 2Q \cdot k_1 - 2Q \cdot k_2$$
$$X = \bar{u}(Q')\gamma_\alpha\{\gamma_\delta\gamma_\mu - g_{\mu\delta}\}v(Q)$$

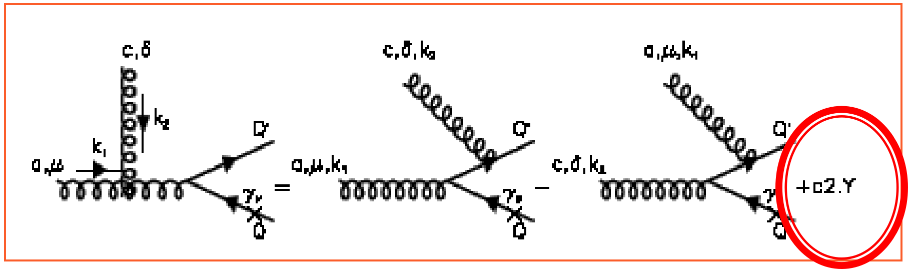

QCD-like → QED-like

$$M^{acd}_{\mu\delta\alpha}(k_1,k_2,Q,Q') \simeq \bar{u}(Q')\Big(\gamma_\delta(\not{Q}'-\not{k}_2+M)\gamma_\mu-\gamma_\mu(\not{Q}'-\not{k}_1+M)\gamma_\delta\Big)\cdot (\not{Q}'-\not{k}_1-\not{k}_2+M)\gamma_\alpha v(Q)+(c2\cdot Y)+\cdots$$

where

$$c2 = m_1^2+m_2^2+2k_1\cdot k_2-2Q'\cdot k_1-2Q'\cdot k_2$$

$$Y = \bar{u}(Q')\{\gamma_\delta\gamma_\mu-g_{\mu\delta}\}\gamma_\alpha v(Q)$$

Note: Extra functions X and Y are from four-gluon-vertex decompasation

All the diagrams can be expressed by its inner structures without introduce extra ones.

A concrete example for decomposing

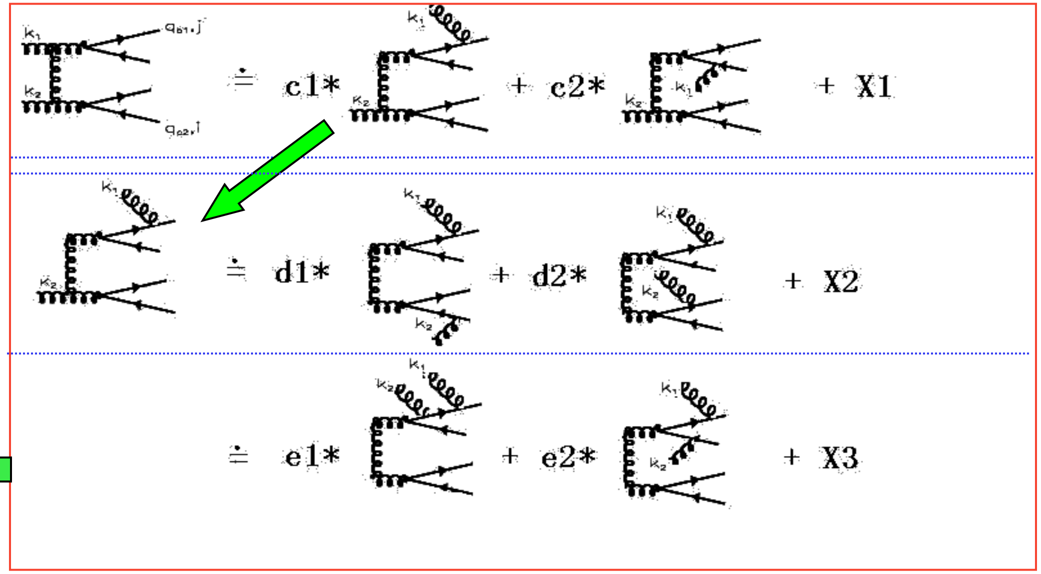

first step

second step

Relations obtained by decomposing

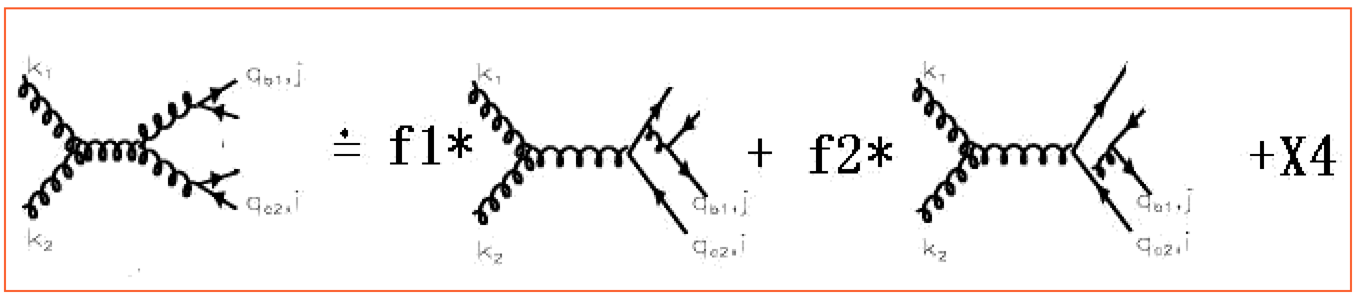

Where (c_i, d_i, e_i, f_i) =±1; X_i can be express by the defined basic function.

D、Amplitude simplification

→ To make program

(A)、general form for the helicity amplitude

$$M_i^{(\lambda_1,\lambda_4,\lambda_5,\lambda_6)}(q_{b1},q_{b2},q_{c1},q_{c2},k_1,k_2) = \sum_{\lambda_2,\lambda_3} C_i X_i D_1 B_{Fi}^{(\lambda_1,\lambda_2,\lambda_3,\lambda_4,\lambda_5,\lambda_6)}(q_{b1},q_{b2},q_{c1},q_{c2},k_1,k_2)\cdot D_2 B_{B_c(B_c^*)}^{(\lambda_2,\lambda_3)}(q_{b2},q_{c1}), \quad (22)$$

Factorization

$$gg \to b+\bar{b}+c+\bar{c}$$
$$c+b \to B_c$$

$$D_2 B_{B_c}^{(\lambda_2,\lambda_3)}(q_{b2},q_{c1}) = \frac{\psi(0)\sqrt{M}}{2\sqrt{m_b m_c}}\delta_{\lambda_2,\lambda_3}(\delta_{\lambda_2-}-\delta_{\lambda_2+}),$$ scalar

Bound state

$$D_2 B_{B_c^*}^{(\lambda_2,\lambda_3)}(q_{b2},q_{c1}) = \frac{\psi(0)\sqrt{M}}{2\sqrt{m_b m_c}}\delta_{\lambda_2,\lambda_3}(\delta_{\lambda_2+}+\delta_{\lambda_2-})\left(\frac{M\epsilon(s_z)\cdot q_0}{P\cdot q_0}\right) + \frac{\psi(0)\sqrt{M}}{2\sqrt{m_b m_c}}\left(\frac{1}{2P\cdot q_0}\right)\langle q_{0\lambda_2}|\not{\epsilon}(s_z)\not{P}|q_{0\lambda_3}\rangle.$$ vector

$$u_s(r) = \frac{1}{\sqrt{2r\cdot q}}(\not{r}+m)|q_h\rangle \qquad \not{\epsilon}^{\pm}(k,q) = \frac{\sqrt{2}}{\langle q_{\mp}|k_{\pm}\rangle}[|k_{\mp}\rangle\langle q_{\mp}|+|q_{\pm}\rangle\langle k_{\pm}|]$$

$$v_s(r) = \frac{1}{\sqrt{2r\cdot q}}(\not{r}-m)|q_{-h}\rangle \qquad \epsilon_{\mu}^{\pm}(k,q) = \langle k_{\pm}|\gamma_{\mu}|q_{\pm}\rangle/\sqrt{2}\langle q_{\mp}|k_{\pm}\rangle$$

(B)、helicity amplitude for the hard scattering process

$E_{m,1,k}$ (m=1-9)

symmetry

$E_{m,j,k}$ (j=1,2,3,4)

combination

B_{Fi}

$$B_{Fi}^{(\lambda_1,\lambda_2,\lambda_3,\lambda_4,\lambda_5,\lambda_6)}(q_{b1},q_{b2},q_{c1},q_{c2},k_1,k_2) \equiv B_{Fi}^{(k)}(q_{b1},q_{b2},q_{c1},q_{c2},k_1,k_2) = \sum_{m=1}^{9}\sum_{j=1}^{4} f_{i,m,j} E_{m,j,k}$$

m-- 9 function

j --4 type of symmetry

k --64 helicity combination

$$E_{m,j,k+16} = +E^{*}_{m,j,k} \; (k=(1,\cdots,4),(9,\cdots,12),(37,\cdots,40),(45,\cdots,48))$$

$$= -E^{*}_{m,j,k} \; (k=(5,\cdots,8),(13,\cdots,16),(33,\cdots,36),(41,\cdots,44))$$

Arrangement for easy programming

TABLE I: The correspondence between $k=1,\cdots,64$ and $\lambda_1=\pm,\lambda_2=\pm,\lambda_3=\pm,\lambda_4=\pm,\lambda_5=\pm,\lambda_6=\pm$, which stand for the helicities of the particles in the process.

k	λ_1	λ_2	λ_3	λ_4	λ_5	λ_6	k	λ_1	λ_2	λ_3	λ_4	λ_5	λ_6	k	λ_1	λ_2	λ_3	λ_4	λ_5	λ_6	k	λ_1	λ_2	λ_3	λ_4	λ_5	λ_6
1	+	+	+	+	+	+	17	−	−	−	−	−	−	33	+	+	−	+	+	+	49	−	−	+	−	−	−
2	+	+	+	+	+	−	18	−	−	−	−	−	+	34	+	+	−	+	+	−	50	−	−	+	−	−	+
3	+	+	+	+	−	+	19	−	−	−	−	+	−	35	+	+	−	+	−	+	51	−	−	+	−	+	−
4	+	+	+	+	−	−	20	−	−	−	−	+	+	36	+	+	−	+	−	−	52	−	−	+	−	+	+
5	+	+	+	−	+	+	21	−	−	−	+	−	−	37	+	+	−	−	+	+	53	−	−	+	+	−	−
6	+	+	+	−	+	−	22	−	−	−	+	−	+	38	+	+	−	−	+	−	54	−	−	+	+	−	+
7	+	+	+	−	−	+	23	−	−	−	+	+	−	39	+	+	−	−	−	+	55	−	−	+	+	+	−
8	+	+	+	−	−	−	24	−	−	−	+	+	+	40	+	+	−	−	−	−	56	−	−	+	+	+	+
9	+	−	−	+	+	+	25	−	+	+	−	−	−	41	+	−	+	+	+	+	57	−	+	−	−	−	−
10	+	−	−	+	+	−	26	−	+	+	−	−	+	42	+	−	+	+	+	−	58	−	+	−	−	−	+
11	+	−	−	+	−	+	27	−	+	+	−	+	−	43	+	−	+	+	−	+	59	−	+	−	−	+	−
12	+	−	−	+	−	−	28	−	+	+	−	+	+	44	+	−	+	+	−	−	60	−	+	−	−	+	+
13	+	−	−	−	+	+	29	−	+	+	+	−	−	45	+	−	+	−	+	+	61	−	+	−	+	−	−
14	+	−	−	−	+	−	30	−	+	+	+	−	+	46	+	−	+	−	+	−	62	−	+	−	+	−	+
15	+	−	−	−	−	+	31	−	+	+	+	+	−	47	+	−	+	−	−	+	63	−	+	−	+	+	−
16	+	−	−	−	−	−	32	−	+	+	+	+	+	48	+	−	+	−	−	−	64	−	+	−	+	+	+

(C)、expansion coefficients

$E_{m,j,k}$

TABLE II: The expansion coefficients $f_{i,m,j}$ for the functions $B^{(k)}_{Fi}(q_{b1}, q_{b2}, q_{c1}, q_{c2}, k_1, k_2)$ which are grouped into the cb subset directly or indirectly through a proper decomposition (the coefficients $f_{i,m,j}$ are not listed here if they are equal to zero in a whole row).

	$j=1$				
m	1	2	3	4	5
$f_{3a,m,j}$	1	0	0	0	0
$f_{3b,m,j}$	0	1	0	0	0
$f_{3d,m,j}$	0	0	1	0	0
$f_{3e,m,j}$	0	0	0	1	0
$f_{4c,m,j}$	-1	0	1	0	$-2(q_{c2}\cdot k_1)$
$f_{4d,m,j}$	0	-1	0	1	$2(q_{c1}\cdot k_1)$
$f_{4f,m,j}$	1	-1	0	0	$2(q_{b1}\cdot k_2)$
$f_{4g,m,j}$	0	0	1	-1	$-2(q_{b2}\cdot k_2)$
$f_{5b,m,j}$	1	-1	-1	1	$s_b+s_c-s_2$

QED-like

One three-gluon vertex

Two three-gluon vertex

cb subset

Gluon exchange

bc subset

TABLE III: The expansion coefficients $f_{i,m,j}$ for the functions $B^{(k)}_{F_i}(q_{b1}, q_{b2}, q_{c1}, q_{c2}, k_1, k_2)$ which are grouped into the cc subset directly or indirectly through a proper decomposition (the coefficients $f_{i,m,j}$, which are equal to zero in a whole row, are not listed here).

	$j=1$					$j=2$				
m	6	7	8	9	5	6	7	8	9	5
$f_{1a,m,j}$	1	0	0	0	0	0	0	0	0	0
$f_{1b,m,j}$	0	0	0	0	0	1	0	0	0	0
$f_{1c,m,j}$	0	1	0	0	0	0	0	0	0	0
$f_{1d,m,j}$	0	0	0	0	0	0	1	0	0	0
$f_{1e,m,j}$	0	0	1	0	0	0	0	0	0	0
$f_{1f,m,j}$	0	0	0	0	0	0	0	1	0	0
$f_{1g,m,j}$	1	0	0	$\frac{f_3}{2}$	0	-1	0	0	$-\frac{f_3}{2}$	0
$f_{1h,m,j}$	0	0	1	$\frac{f_4}{2}$	$2f_4$	0	0	-1	$\frac{f_4}{2}$	$-2f_4$
$f_{4a,m,j}$	-1	1	0	$2q_{c2}\cdot k_2$	0	0	0	0	0	$-2q_{c2}\cdot k_2$
$f_{4b,m,j}$	0	0	0	0	$4q_{c1}\cdot k_2$	0	-1	1	$-2q_{c1}\cdot k_2$	$-2q_{c1}\cdot k_2$
$f_{4c,m,j}$	0	0	0	0	$-2q_{c2}\cdot k_1$	-1	1	0	$2q_{c2}\cdot k_1$	0
$f_{4d,m,j}$	0	-1	1	$-2q_{c1}\cdot k_1$	$-2q_{c1}\cdot k_1$	0	0	0	0	$4q_{c1}\cdot k_2$
$f_{5a,m,j}$	1	-1	0	$2q_{c2}\cdot k_2$	$-4q_{c1}\cdot k_2$	0	-1	1	$2q_{c1}\cdot k_2$	f_1
$f_{5b,m,j}$	0	-1	1	$2q_{c1}\cdot k_1$	f_2	1	-1	0	$2q_{c2}\cdot k_1$	$-4q_{c1}\cdot k_1$
$f_{5c,m,j}$	-1	0	1	$-\frac{f_3-f_4}{2}$	$2f_4$	1	0	-1	$\frac{f_3-f_4}{2}$	$-2f_4$
$f_{5d1,m,j}$	0	0	0	0	1	0	0	0	0	-1
$f_{5d2,m,j}$	0	0	0	$\frac{1}{2}$	0	0	0	0	$\frac{1}{2}$	-1
$f_{5d3,m,j}$	0	0	0	$\frac{1}{2}$	-1	0	0	0	$\frac{1}{2}$	0

QED-like

one three-gluon vertex

two three-gluon vertex

four-gluon vertex

cc subset

quark exchange

bb subset

(D)、basic functions $E_{m,j,k}(q_{b1}, q_{b2}, q_{c1}, q_{c2}, k_1, k_2)$ ⟵ Basic diagram

a) eight fermion lines (f_i)。 (q_0— light-like reference momentum)

$$
\begin{aligned}
f_0(q_1, q_2, \lambda_1, \lambda_2) &= \langle q_{0\lambda_1}|(\not{q}_1 + m)\gamma_\delta(\not{q}_2 - m)|q_{0\lambda_2}\rangle \\
f_1(q_1, q_2, k, \lambda_1, \lambda_2, \lambda_3) &= \langle q_{0\lambda_1}|(\not{q}_1 + m)\gamma_\delta(\not{k} - \not{q}_2 + m)\not{\epsilon}^{\lambda_3}(k, q_0)(\not{q}_2 - m)|q_{0\lambda_2}\rangle \\
f_2(q_1, q_2, k, \lambda_1, \lambda_2, \lambda_3) &= \langle q_{0\lambda_1}|(\not{q}_1 + m)\not{\epsilon}^{\lambda_3}(k, q_0)(\not{q}_1 - \not{k} + m)\gamma_\delta(\not{q}_2 - m)|q_{0\lambda_2}\rangle \\
f_3(q_1, q_2, k, \lambda_1, \lambda_2, \lambda_3) &= \langle q_{0\lambda_1}|(\not{q}_1 + m)\not{\epsilon}^{\lambda_3}(k, q_0)(\not{q}_2 - m)|q_{0\lambda_2}\rangle \\
f_4(q_1, q_2, k_1, k_2, \lambda_1, \lambda_2, \lambda_3, \lambda_4) &= \langle q_{0\lambda_1}|(\not{q}_1 + m)\gamma_\delta(\not{k}_1 + \not{k}_2 - \not{q}_2 + m)\not{\epsilon}^{\lambda_3}(k_1, q_0) \\
&\quad (\not{k}_2 - \not{q}_2 + m)\not{\epsilon}^{\lambda_4}(k_2, q_0) \cdot (\not{q}_2 - m)|q_{0\lambda_2}\rangle \\
f_5(q_1, q_2, k_1, k_2, \lambda_1, \lambda_2, \lambda_3, \lambda_4) &= \langle q_{0\lambda_1}|(\not{q}_1 + m)\not{\epsilon}^{\lambda_3}(k_1, q_0)(\not{q}_1 - \not{k}_1 + m)\gamma_\delta \\
&\quad (\not{k}_2 - \not{q}_2 + m)\not{\epsilon}^{\lambda_4}(k_2, q_0) \cdot (\not{q}_2 - m)|q_{0\lambda_2}\rangle \\
f_6(q_1, q_2, k_1, k_2, \lambda_1, \lambda_2, \lambda_3, \lambda_4) &= \langle q_{0\lambda_1}|(\not{q}_1 + m)\not{\epsilon}^{\lambda_3}(k_1, q_0)(\not{q}_1 - \not{k}_1 + m)\not{\epsilon}^{\lambda_4}(k_2, q_0) \\
&\quad (\not{q}_1 - \not{k}_1 - \not{k}_2 + m)\gamma_\delta \cdot (\not{q}_2 - m)|q_{0\lambda_2}\rangle \\
f_7(q_1, q_2, k_1, k_2, \lambda_1, \lambda_2, \lambda_3, \lambda_4) &= \langle q_{0\lambda_1}|(\not{q}_1 + m)\gamma_\delta\not{\epsilon}^{\lambda_3}(k_1, q_0)\not{\epsilon}^{\lambda_4}(k_2, q_0)(\not{q}_2 - m)|q_{0\lambda_2}\rangle
\end{aligned}
$$

b) definition of the nine basic functions

7+2

$$E_{1,1,k} = f_1(q_{c1}, q_{c2}, k_1, \lambda_3, \lambda_4, \lambda_5) \cdot f_2(q_{b1}, q_{b2}, k_2, \lambda_1, \lambda_2, \lambda_6),$$
$$E_{2,1,k} = f_2(q_{c1}, q_{c2}, k_1, \lambda_3, \lambda_4, \lambda_5) \cdot f_2(q_{b1}, q_{b2}, k_2, \lambda_1, \lambda_2, \lambda_6),$$
$$E_{3,1,k} = f_1(q_{c1}, q_{c2}, k_1, \lambda_3, \lambda_4, \lambda_5) \cdot f_1(q_{b1}, q_{b2}, k_2, \lambda_1, \lambda_2, \lambda_6),$$
$$E_{4,1,k} = f_2(q_{c1}, q_{c2}, k_1, \lambda_3, \lambda_4, \lambda_5) \cdot f_1(q_{b1}, q_{b2}, k_2, \lambda_1, \lambda_2, \lambda_6),$$
$$E_{5,1,k} = f_3(q_{b1}, q_{b2}, k_2, \lambda_1, \lambda_2, \lambda_5) \cdot f_3(q_{c1}, q_{c2}, k_1, \lambda_3, \lambda_4, \lambda_6),$$
$$E_{6,1,k} = f_0(q_{b1}, q_{b2}, \lambda_1, \lambda_2) \cdot f_4(q_{c1}, q_{c2}, k_1, k_2, \lambda_3, \lambda_4, \lambda_5, \lambda_6),$$
$$E_{7,1,k} = f_0(q_{b1}, q_{b2}, \lambda_1, \lambda_2) \cdot f_5(q_{c1}, q_{c2}, k_1, k_2, \lambda_3, \lambda_4, \lambda_5, \lambda_6),$$
$$E_{8,1,k} = f_0(q_{b1}, q_{b2}, \lambda_1, \lambda_2) \cdot f_6(q_{c1}, q_{c2}, k_1, k_2, \lambda_3, \lambda_4, \lambda_5, \lambda_6),$$
$$E_{9,1,k} = f_0(q_{b1}, q_{b2}, \lambda_1, \lambda_2) \cdot f_7(q_{c1}, q_{c2}, k_1, k_2, \lambda_3, \lambda_4, \lambda_5, \lambda_6).$$

c) relations between these basic functions

symmetries

$$E_{1,3,k} = E_{4,2,k},\ E_{2,3,k} = E_{2,2,k},\ E_{3,3,k} = E_{3,2,k},$$
$$E_{4,3,k} = E_{1,2,k},\ E_{5,3,k} = E_{5,2,k},\ E_{1,4,k} = E_{4,1,k},$$
$$E_{2,4,k} = E_{2,1,k},\ E_{3,4,k} = E_{3,1,k},\ E_{4,4,k} = E_{1,1,k},$$
$$E_{5,4,k} = E_{5,1,k},\ E_{9,4,k} = E_{9,1,k} + E_{9,2,k} - E_{9,3,k}.$$

Two independent functions

decompose

$$E_{6,1,k} = E_{7,1,k} + 2q_{c2} \cdot k_2 E_{9,1,k} - E_{3,2,k} + E_{1,2,k} \,,$$
$$E_{6,2,k} = E_{7,2,k} + 2q_{c2} \cdot k_1 E_{9,2,k} - E_{3,1,k} + E_{1,1,k} \,,$$
$$E_{6,3,k} = E_{7,3,k} + 2q_{b2} \cdot k_2 E_{9,3,k} - E_{3,4,k} + E_{1,4,k} \,,$$
$$E_{6,4,k} = E_{7,4,k} + 2q_{c2} \cdot k_1 E_{9,4,k} - E_{3,3,k} + E_{1,3,k} \,;$$

$$E_{7,1,k} = -E_{4,1,k} + E_{2,1,k} + E_{8,1,k} - 2q_{c1} \cdot k_1 (2E_{5,1,k} - 2E_{5,2,k} + E_{9,1,k})$$
$$E_{7,2,k} = -E_{4,2,k} + E_{2,2,k} + E_{8,2,k} - 2q_{c1} \cdot k_2 (2E_{5,2,k} - 2E_{5,1,k} + E_{9,2,k})$$
$$E_{7,3,k} = -E_{4,3,k} + E_{2,3,k} + E_{8,3,k} - 2q_{b1} \cdot k_1 (2E_{5,3,k} - 2E_{5,4,k} + E_{9,3,k})$$
$$E_{7,4,k} = -E_{4,4,k} + E_{2,4,k} + E_{8,4,k} - 2q_{b1} \cdot k_2 (2E_{5,4,k} - 2E_{5,3,k} + E_{9,4,k})$$

(E)、Color rearrangement

$$M^{(\lambda_1,\lambda_4,\lambda_5,\lambda_6)}(q_{b1},q_{b2},q_{c1},q_{c2},k_1,k_2) = \sum_{i=1}^{36} M_i^{(\lambda_1,\lambda_4,\lambda_5,\lambda_6)}(q_{b1},q_{b2},q_{c1},q_{c2},k_1,k_2)$$
$$= \sum_{m=1}^{5} C_{mij} M_m'^{(\lambda_1,\lambda_4,\lambda_5,\lambda_6)}(q_{b1},q_{b2},q_{c1},q_{c2},k_1,k_2)$$

where

$$M'_m = \sum_{\lambda_2,\lambda_3} M_{Fm}'^{(\lambda_1,\lambda_2,\lambda_3,\lambda_4,\lambda_5,\lambda_6)}(q_{b1},q_{b2},q_{c1},q_{c2},k_1,k_2) D_2 B_B^{(\lambda_2,\lambda_3)}(q_{b2},q_{c1})$$

M'_{Fm} can be obtained by adding the scalar part of the propagator to the above obtained one.

$$\begin{aligned} M'_{F1} = \frac{D_1}{2}\Big(& 2(X_{3a}+X_{4c}+X_{5b})E_{1,1,k} - 2X_{4e}E_{2,4,k} - 2X_{4c}E_{3,1,k} + 2X_{4e}E_{4,4,k} \\ & -X_{5d}(2E_{5,1,k} - 4E_{5,2,k} + E_{9,1,k} + E_{9,2,k}) + 2\{-(X_{1g}+X_{5c})E_{6,1,k} \\ & +(X_{1b}+X_{1g}+X_{5c})E_{6,2,k} + X_{5c}(E_{8,1,k} - E_{8,2,k}) - X_{2h}E_{8,3,k} + \\ & (X_{2f}+X_{2h})E_{8,4,k} + 2X_{4e}E_{5,4,k}q_{b1}\cdot k_2\} + 4X_{4c}E_{5,1,k}q_{c2}\cdot k_1 - (X_{1g} + \\ & X_{5c})(E_{9,1,k} - E_{9,2,k})f_3 + X_{5c}(4E_{5,1,k} - 4E_{5,2,k} + E_{9,1,k} - \\ & E_{9,2,k})f_4 + X_{2h}(-4E_{5,3,k} + 4E_{5,4,k} - E_{9,3,k} + E_{9,4,k})f_6 - \\ & 2X_{5b}\{E_{2,1,k} + E_{3,1,k} - E_{4,1,k} - E_{5,1,k}(s_c - s_1 + s_b)\}\Big), \end{aligned}$$

$$
\begin{aligned}
M'_{F2} = \; & \frac{D_1}{2}\Big(2(X_{3e} + X_{4a} + X_{5a})E_{1,2,k} - 2X_{4g}E_{2,3,k} - 2X_{4a}E_{3,2,k} + \\
& 2((X_{1a} + X_{1g} + X_{5c})E_{6,1,k} - (X_{1g} + X_{5c})E_{6,2,k} + X_{5c}(E_{8,2,k} - \\
& E_{8,1,k}) + (X_{2e} + X_{2h})E_{8,3,k} - X_{2h}E_{8,4,k}) - X_{5d}(2E_{5,2,k} + \\
& E_{9,1,k} + E_{9,2,k}) + 2X_{4g}(E_{4,3,k} + 2E_{5,3,k}q_{b1} \cdot k_1) + \\
& 4X_{4a}E_{5,2,k}q_{c2} \cdot k_2 + (X_{1g} + X_{5c})(E_{9,1,k} - E_{9,2,k})f_3 + \\
& X_{5c}(4E_{5,2,k} - E_{9,1,k} + E_{9,2,k})f_4 + 4E_{5,1,k} \cdot (X_{5d} - X_{5c}f_4) + \\
& X_{2h}(4E_{5,3,k} - 4E_{5,4,k} + E_{9,3,k} - E_{9,4,k})f_6 - 2X_{5a}(E_{2,2,k} \\
& + E_{3,2,k} - E_{4,2,k} - E_{5,2,k}(-s_2 + s_b + s_c))\Big),
\end{aligned}
$$

$$
\begin{aligned}
M'_{F3} = \; & \frac{D_1}{2}\Big(- 2(X_{4c} + X_{5b})E_{1,1,k} + 2X_{4e}E_{2,4,k} + 2(X_{3c} + X_{4c})E_{3,1,k} + \\
& 2X_{3d}E_{4,1,k} + 2(X_{5c}E_{6,1,k} - X_{5c}E_{6,2,k} + X_{2a}E_{6,4,k} + \\
& X_{2g}(-E_{6,3,k} + E_{6,4,k}) + X_{1d}E_{7,2,k} + X_{2d}E_{7,4,k} - \\
& (X_{1h} + X_{5c})E_{8,1,k} + (X_{1f} + X_{1h} + X_{5c})E_{8,2,k}) + X_{5d}(2E_{5,1,k} - \\
& 4E_{5,2,k} + E_{9,1,k} + E_{9,2,k}) - 2X_{4e}(E_{4,4,k} + 2E_{5,4,k}q_{b1} \cdot k_2) \\
& -4X_{4c}E_{5,1,k}q_{c2} \cdot k_1 + X_{5c}(E_{9,1,k} - E_{9,2,k})f_3 - (X_{1h} + X_{5c}) \cdot \\
& (4E_{5,1,k} - 4E_{5,2,k} + E_{9,1,k} - E_{9,2,k})f_4 - X_{2g}(E_{9,3,k} - \\
& E_{9,4,k})f_5 + 2((X_{3b} + X_{5b})E_{2,1,k} + X_{5b}(E_{3,1,k} - E_{4,1,k} - \\
& E_{5,1,k}(-s_1 + s_b + s_c)))\Big),
\end{aligned}
$$

$$
\begin{aligned}
M'_{F4} &= \frac{D_1}{2}\Big(-2(X_{4a}+X_{5a})E_{1,2,k}+2(X_{3g}+X_{4a})E_{3,2,k}+2X_{3h}E_{4,2,k}- \\
&2X_{5c}E_{6,1,k}+2(X_{5c}E_{6,2,k}+(X_{2a}+X_{2g})E_{6,3,k}-X_{2g}E_{6,4,k}+ \\
&X_{1c}E_{7,1,k}+X_{2c}E_{7,3,k}+(X_{1e}+X_{1h}+X_{5c})E_{8,1,k} \\
&-(X_{1h}+X_{5c})E_{8,2,k})+X_{5d}(2E_{5,2,k}+E_{9,1,k} \\
&+E_{9,2,k})+2X_{4g}(E_{2,3,k}-E_{4,3,k}-2E_{5,3,k}q_{b1}\cdot k_1) \\
&-4X_{4a}E_{5,2,k}q_{c2}\cdot k_2-X_{5c}(E_{9,1,k}E_{9,2,k})f_3- \\
&(X_{1h}+X_{5c})(4E_{5,2,k}-E_{9,1,k}+E_{9,2,k})f_4+4E_{5,1,k}(-X_{5d}+ \\
&(X_{1h}+X_{5c})f_4)+X_{2g}(E_{9,3,k}-E_{9,4,k})f_5+2((X_{3f}+X_{5a})E_{2,2,k} \\
&+X_{5a}(E_{3,2,k}-E_{4,2,k}-E_{5,2,k}(-s_2+s_b+s_c)))\Big)\,,
\end{aligned}
$$

$$
\begin{aligned}
M'_{F5} &= D_1\Big(-(X_{5b}E_{1,1,k})+(X_{4d}+X_{5b})E_{2,1,k}-(X_{3d}+X_{4d})E_{4,1,k}- \\
&X_{3h}E_{4,2,k}-X_{2a}(E_{6,3,k}+E_{6,4,k})-X_{1e}E_{8,1,k}-X_{1f}E_{8,2,k} \\
&-X_{5d}(E_{5,1,k}+E_{5,2,k}-E_{9,1,k}-E_{9,2,k})+X_{4h}(-E_{1,3,k}+ \\
&E_{3,3,k}-2E_{5,3,k}q_{b2}\cdot k_1)+X_{4f}(-E_{1,4,k}+E_{3,4,k}- \\
&2E_{5,4,k}q_{b2}\cdot k_2)-2X_{4d}E_{5,1,k}q_{c1}\cdot k_1+X_{4b}(E_{2,2,k}-E_{4,2,k}- \\
&2E_{5,2,k}q_{c1}\cdot k_2)-X_{5b}(-E_{3,1,k}+E_{4,1,k}+ \\
&E_{5,1,k}(-s_1+s_b+s_c))-X_{5a}(E_{1,2,k}-E_{2,2,k}-E_{3,2,k}+ \\
&E_{4,2,k}+E_{5,2,k}(-s_2+s_b+s_c)))\,,
\end{aligned}
$$

$$|M^{(\lambda_1,\lambda_4,\lambda_5,\lambda_6)}(q_{b1},q_{b2},q_{c1},q_{c2},k_1,k_2)|^2 = \frac{4}{27}|8M'_1-M'_3|^2+\frac{4}{27}|8M'_2-M'_4|^2- \frac{1}{27}|(8M'_1-M'_3)\cdot(8M'_2-M'_4)|+\frac{3}{2}|M'_5|^2 -\frac{1}{3}|(8M'_1+8M'_2-M'_3-M'_4)M'_5|$$

Square of the amplitude:

$$|M|^2=\sum_{\lambda_1=\pm}\sum_{\lambda_4=\pm}\sum_{\lambda_5=\pm}\sum_{\lambda_6=\pm}|M^{(\lambda_1,\lambda_4,\lambda_5,\lambda_6)}(q_{b1},q_{b2},q_{c1},q_{c2},k_1,k_2)|^2$$

(F)、phase space integration

cross section for the subprocess

$$d\hat{\sigma}=\frac{1}{2^{11}\times 3}\frac{(2\pi)^4|M|^2}{4(k_1\cdot k_2)}\times d\Phi_3(k_1+k_2;P,q_{b1},q_{c2}),$$

RAMBOS

VEGAS

two to three body phase space

$$d\Phi_3(k_1+k_2;P,q_{b1},q_{c2})=\delta^4(k_1+k_2-P-q_{b1}-q_{c2})\frac{d^3\vec{\mathbf{P}}}{(2\pi)^3 2E_P}\frac{d^3\vec{\mathbf{q}}_{b1}}{(2\pi)^3 2E_{q_{b1}}}\frac{d^3\vec{\mathbf{q}}_{c2}}{(2\pi)^3 2E_{q_{c2}}}.$$

BCVEGPY - program

Whole flowchart

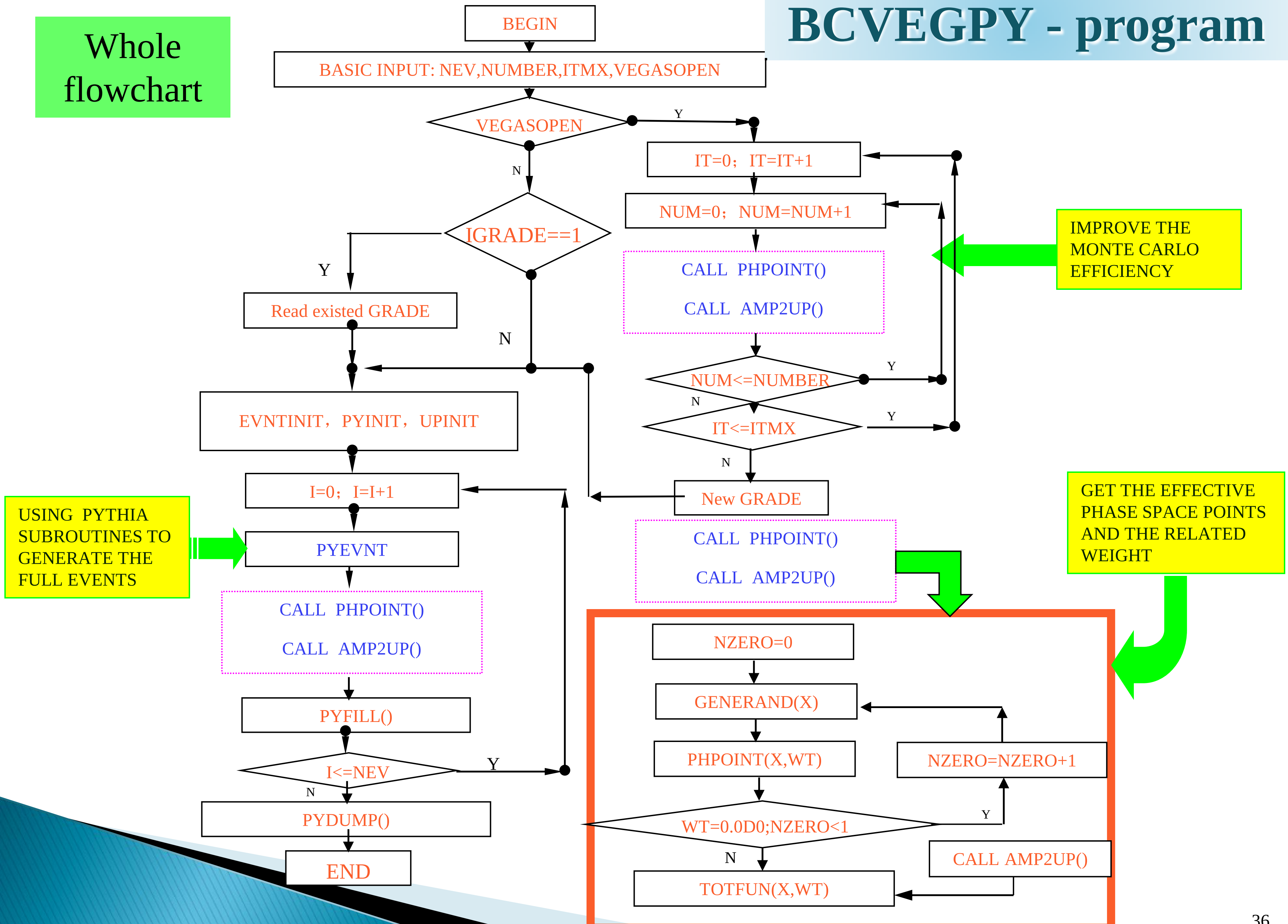

Color flow for different processes

Color-flow decomposition derived by taking the large N_c limit

PYTHIA
LUND Model

PHYSICAL REVIEW D 67, 014026 (2003)

Color-flow decomposition of QCD amplitudes

F. Maltoni,[1] K. Paul,[1] T. Stelzer,[1] and S. Willenbrock[1,2]

Color flow

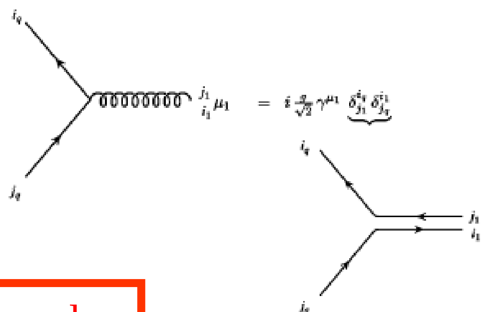

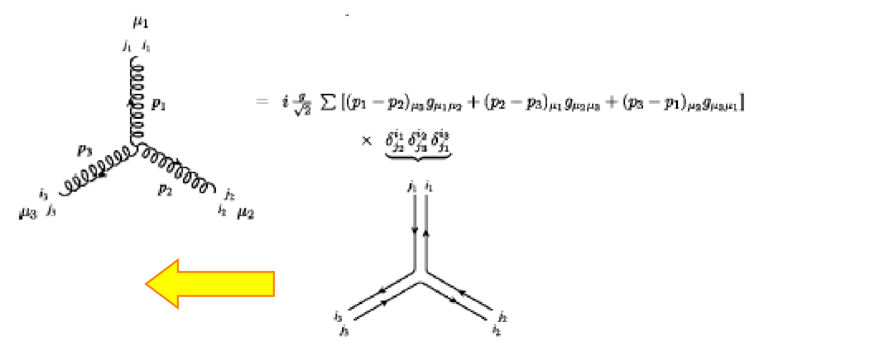

Feynman rules for color-flow In large Nc limie

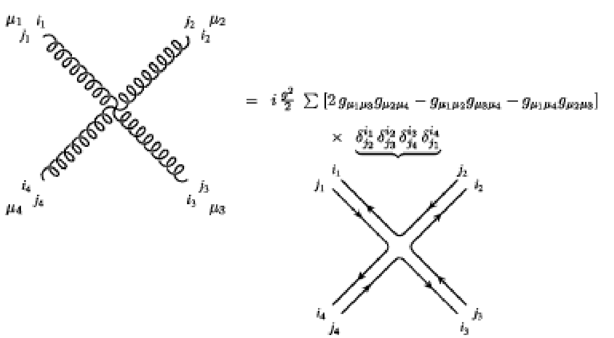

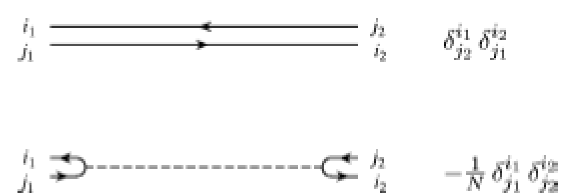

Bc-meson color-flow probability

Partial amplitude (or color-ordered amplitude)-----whose square is just the probability for a particular color-flow. It is the same for 3-different decomposition schemes (fundamental-, adjoint-representation, color-flow decomposition)—demonstrated in PRD67,014026(2003)

Color-singlet:

$$M = (T^a T^b)_{ij} M_1 + (T^b T^a)_{ij} M_2 + (\delta_{ij} Tr[T^a T^b]) M_3,$$

Color-octet:

$$\begin{aligned} M \;=\; & (T^b T^a T^d)_{ij} M_1 + (T^a T^b T^d)_{ij} M_2 + (T^b_{ij} Tr[T^a T^d]) M_3 + (T^a_{ij} Tr[T^b T^d]) M_4 \\ & + (\delta_{ij} Tr[T^b T^a T^d]) M_5 + (\delta_{ij} Tr[T^a T^b T^d]) M_6 + (T^d T^b T^a)_{ij} M_7 + (T^d T^a T^b)_{ij} M_8 \\ & + (T^a T^d T^b)_{ij} M_9 + (T^b T^d T^a)_{ij} M_{10}. \end{aligned}$$

$$gg \to (c\bar{b})_1 + b + \bar{c}$$

For the color-singlet production processes, there are totally three independent color-flows

Equivalent

$$c_1 = (\delta^{j}_{i_2}\delta^{j_2}_{i_1}\delta^{j_1}_{i}),\quad c_2 = (\delta^{j}_{i_1}\delta^{j_1}_{i_2}\delta^{j_2}_{i}),\quad c_3 = (\delta^{j}_{i}\delta^{j_2}_{i_1}\delta^{j_1}_{i_2}),$$

$$c_1 \to (T^aT^b)_{ij},\quad c_2 \to (T^bT^a)_{ij},\quad c_3 \to (\delta_{ij}Tr[T^aT^b]).$$

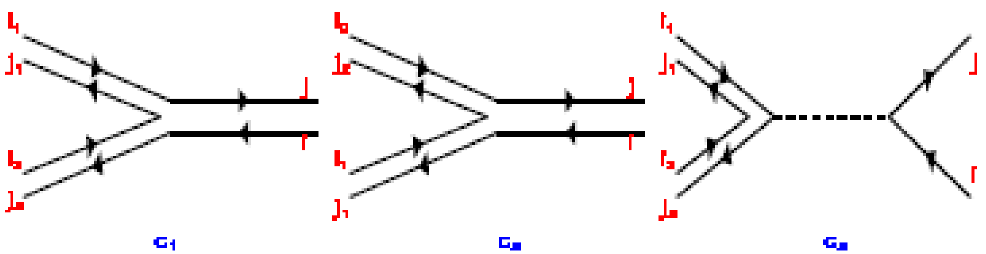

FIG. 1: Color flow diagrams for the color-singlet case based on the color-flow decomposition[11]. Each pair of indices i_k and j_k corresponds to an external gluon, i.e. $k = 1$ is for gluon-1 and $k = 2$ for gluon-2. i and j are the decomposed color indices for the outgoing $\bar{c}$ and b respectively.

$$gg \to (c\bar{b})_8 + b + \bar{c}$$

For the color-octet production processes, there are totally ten independent color-flows

$$c_1 = (\delta_i^{j_2}\delta_{i_2}^{j_1}\delta_{i_1}^{j_3}\delta_{i_3}^{j}),\ c_2 = (\delta_i^{j_1}\delta_{i_1}^{j_2}\delta_{i_2}^{j_3}\delta_{i_3}^{j}),\ c_3 = (\delta_{i_1}^{j_3}\delta_{i_3}^{j_1}\delta_i^{j_2}\delta_{i_2}^{j}),$$

$$c_4 = (\delta_{i_2}^{j_3}\delta_{i_3}^{j_2}\delta_i^{j_1}\delta_{i_1}^{j}),\ c_5 = (\delta_i^{j}\delta_{i_2}^{j_1}\delta_{i_1}^{j_3}\delta_{i_3}^{j_2}),\ c_6 = (\delta_i^{j}\delta_{i_1}^{j_2}\delta_{i_2}^{j_3}\delta_{i_3}^{j_1}),$$

$$c_7 = (\delta_i^{j_3}\delta_{i_3}^{j_2}\delta_{i_2}^{j_1}\delta_{i_1}^{j}),\ c_8 = (\delta_i^{j_3}\delta_{i_3}^{j_1}\delta_{i_1}^{j_2}\delta_{i_2}^{j}),\ c_9 = (\delta_i^{j_1}\delta_{i_1}^{j_3}\delta_{i_3}^{j_2}\delta_{i_2}^{j}),\ c_{10} = (\delta_i^{j_2}\delta_{i_2}^{j_3}\delta_{i_3}^{j_1}\delta_{i_1}^{j}),$$

Equivalent

$$c_1 \to (T^bT^aT^d)_{ij},\ \ c_2 \to (T^aT^bT^d)_{ij},\ \ c_3 \to (T^b_{ij}Tr[T^aT^d]),$$

$$c_4 \to (T^a_{ij}Tr[T^bT^d]),\ \ c_5 \to (\delta_{ij}Tr[T^bT^aT^d]),\ \ c_6 \to (\delta_{ij}Tr[T^aT^bT^d]),$$

$$c_7 \to (T^dT^bT^a)_{ij},\ \ c_8 \to (T^dT^aT^b)_{ij},\ \ c_9 \to (T^aT^dT^b)_{ij},\ \ c_{10} \to (T^bT^dT^a)_{ij},$$

Exchange the color indices

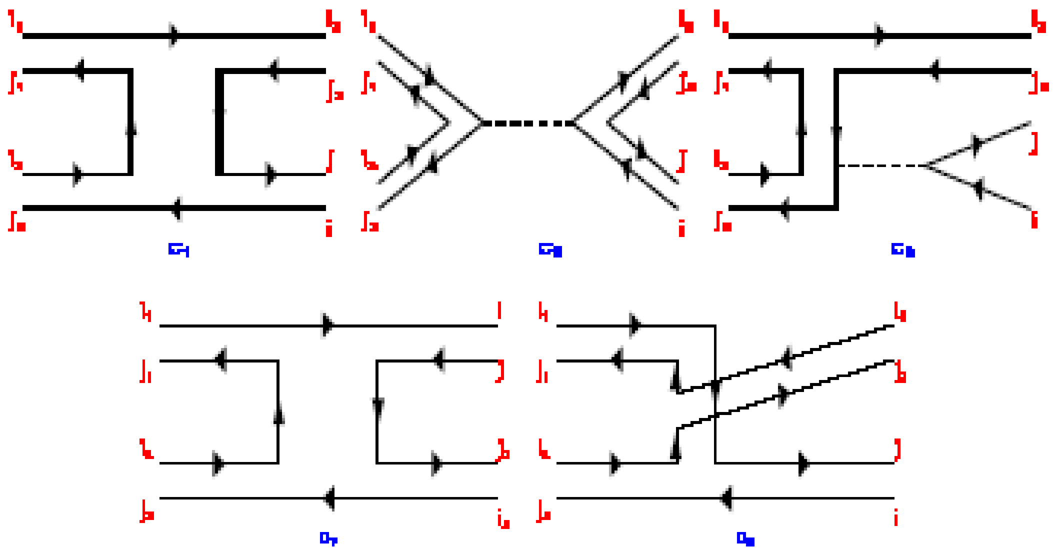

FIG. 2: Color flow diagrams for the color-octet case based on the color-flow decomposition[11]. Each pair of indices i_k and j_k corresponds to an external gluon, i.e. $k = 1$ is for gluon-1, $k = 2$ for gluon-2 and $k = 3$ for the color-octet $(c\bar{b})$-quarkonium. i and j are the decomposed color indices for the outgoing $\bar{c}$ and b respectively. The diagrams for c_{n+1} $(n = 1, 2, \cdots, 5)$ can be directly obtained by gluon exchange.

The cross-terms are suppressed by powers of N_c and can be safely neglected in the large N_c limit.---at least $1/N^2_c$

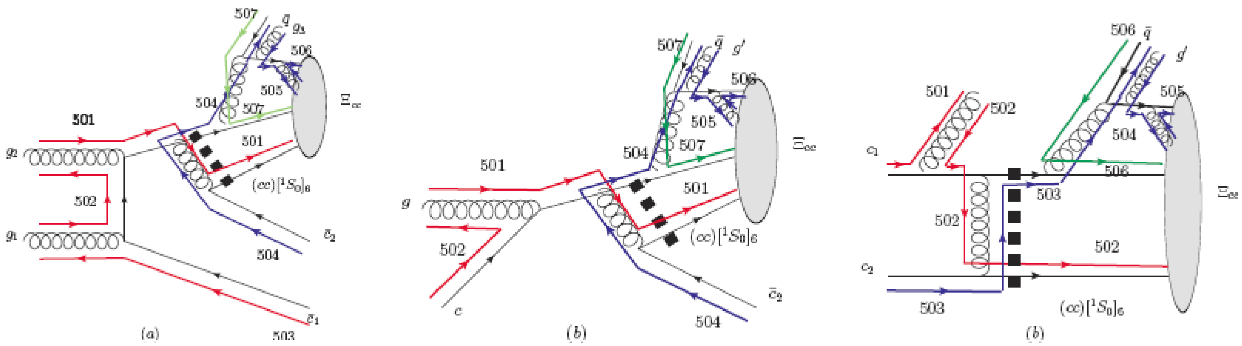

FIG. 2: (Color on line) Typical color flow for gluon-gluon fusion mechanism (Left), gluon-charm collision mechanism (Middle) and charm-charm collision mechanism (Right), where the thick dashed line shows the corresponding intermediate diquark state $(cc)[^1S_0]_6$. Three colorful lines are for color flow lines according to PYTHIA naming rules.

Typical color flow for g+g->Xicc (3s1)

$[0,503] \to [502,503] \to [501,502] \to [501,0] \to$ colorless bound state $\Xi_{cc}^{+,++}/\Omega_{cc}^{+}$,

$[0,504] \to [504,0] \to$ colorless bound state $\Xi_{cc}^{+,++}/\Omega_{cc}^{+}$,

$[0,505] \to [505,0] \to$ colorless bound state $\Xi_{cc}^{+,++}/\Omega_{cc}^{+}$, PYTHIA8.0 solve the problem of color flow

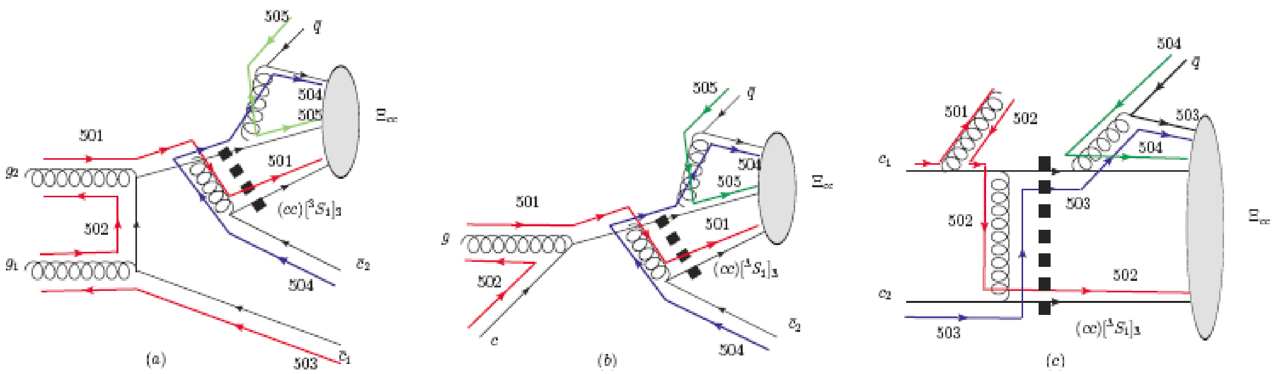

FIG. 1: (Color on line) Typical color flow for gluon-gluon fusion mechanism (Left), gluon-charm collision mechanism (Middle) and charm-charm collision mechanism (Right), where the thick dashed line shows the corresponding intermediate diquark state $(cc)[^3S_1]_{\bar{3}}$. Three colorful lines are for color flow lines according to PYTHIA naming rules.

Typical color flow for g+g->Xicc (3s1)

$[0, 503] \to [502, 503] \to [501, 502] \to [501, 0] \to$ **colorless bound state** $\Xi_{\mathbf{cc}}^{+;++}/\Omega_{cc}^{+}$,

$[0, 504] \to [504, 0] \to$ **colorless bound state** $\Xi_{\mathbf{cc}}^{+;++}/\Omega_{cc}^{+}$,

$[0, 505] \to [505, 0] \to$ **colorless bound state** $\Xi_{\mathbf{cc}}^{+;++}/\Omega_{cc}^{+}$,

A cross-check

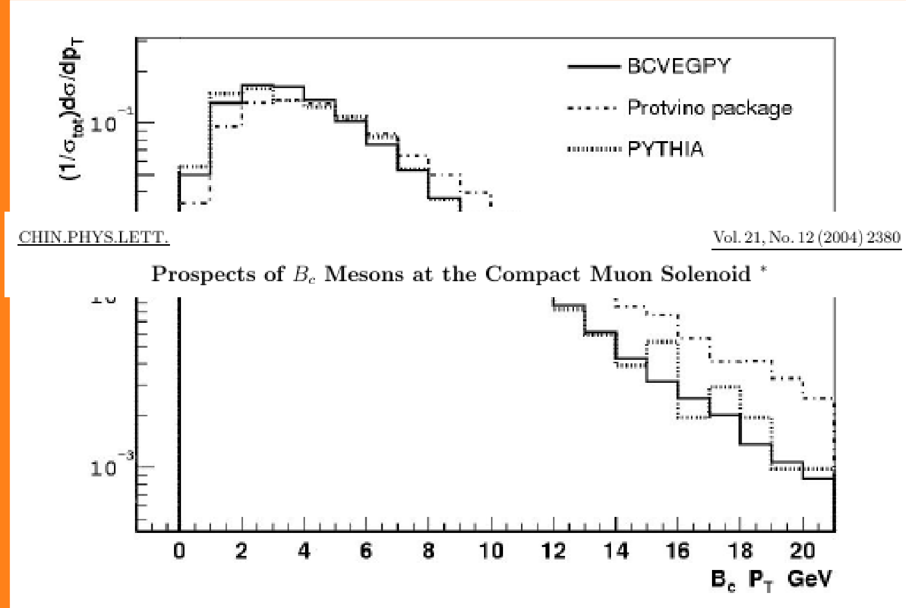

CHIN.PHYS.LETT. Vol. 21, No. 12 (2004) 2380

Prospects of B_c Mesons at the Compact Muon Solenoid *

Table 4

Comparison of total cross sections for $gg \to B_c(B_c^*) + b + \bar{c}$ with th
parameters are $m_b = 4.9$ GeV, $m_c = 1.5$ GeV, $M_{B_c^*} = m_b + m_c$, f_{B_c}
parenthesis shows the Monte Carlo uncertainty in the last digit. The

$\sqrt{s}$	20 GeV	30 Ge	Ge V
σ_{B_c}	$0.6579(5) \times 10^{-2}$	$0.9465(8) \times 10^{-2}$	$0.7872(8) \times 10^{-2}$
σ_{B_c} [7]	$0.661(7) \times 10^{-2}$	$0.949(8) \times 10^{-2}$	$0.782(9) \times 10^{-2}$
$\sigma_{B_c^*}$	$0.1606(1) \times 10^{-1}$	$0.2460(3) \times 10^{-1}$	$0.2033(2) \times 10^{-1}$
$\sigma_{B_c^*}$ [7]	$0.160(2) \times 10^{-1}$	$0.244(3) \times 10^{-1}$	$0.203(3) \times 10^{-1}$

Table 5

Comparison of total cross sections for $gg \to B_c + b + \bar{c}$ with the corresponding results of Ref. [8]. The input parameters are $m_b = 3m_c$, $M_{B_c} = 6.30$ GeV, $f_{B_c} = 0.480$ GeV, $\alpha_s = 0.2$. The number in parenthesis shows the Monte Carlo uncertainty in the last digit. The cross sections are expressed in nb

$\sqrt{s}$	20 GeV	30 GeV	60 GeV	80 GeV
σ_{B_c}	$0.6853(5) \times 10^{-2}$	$0.9731(8) \times 10^{-2}$	$0.7997(9) \times 10^{-2}$	$0.6244(9) \times 10^{-2}$
σ_{B_c} [8]	$0.686(2) \times 10^{-2}$	$0.971(4) \times 10^{-2}$	$0.793(5) \times 10^{-2}$	$0.623(5) \times 10^{-2}$

Computer Physics Communications 159 (2004) 192–224

Improve the efficiency for unweighted events by using BCVEGPY and GENXICC

Weighted events : (IDWTUP=3) – time-saving – no waste events

All partonic events are accepted by PYTHIA with unit weight (100% pass): two ways

A) The **phase-space are uniformly generated**.

B) **VEGAS** is adopted to generate sampling importance function to improve its accuracy.

The phase-space are generated according to the relative importance of this point.

Then, one can use the weight of each points to restore total CS or distributions.

Unweighted events : (IDWTUP=1) – time-consuming – less waste events more better

A) Using PYTHIA inner hit-and-miss technology (von Neumann algorithm):

XWGTUP/XMAXUP ≥ PYR(0) accept

XWGTUP/XMAXUP < PYR(0) reject

B) Using improved hit-and-miss technology:

MINT, divided into mesh grade, XMAXUP to be a group, pass the criteria much more effectively

Summary and Prospects

- **Due to its high efficiency, BCVEGPY and GENXICC, are very useful for MC simulation and also for theoretical studies.**

- **Now it has been adopted by ATLAS, CMS, LHCb, CDF and D0 groups respectively.**

- **The coming LHC experiment shall provide a better platform to check all the theoretical predications and to learn the Bc, Xicc, Xibc, Xibb properties in more detail.**

- **The programmed super Z factory, GIGAZ, LEP3, and etc. shall provide other platforms for doubly heavy meson and baryon productions, which are in progress. Especially, a generator BEEC shall be available soon.**

Backup slides for BCVEGPY and GENXICC applications

some results for the S-wave Bc production

Uncertainties

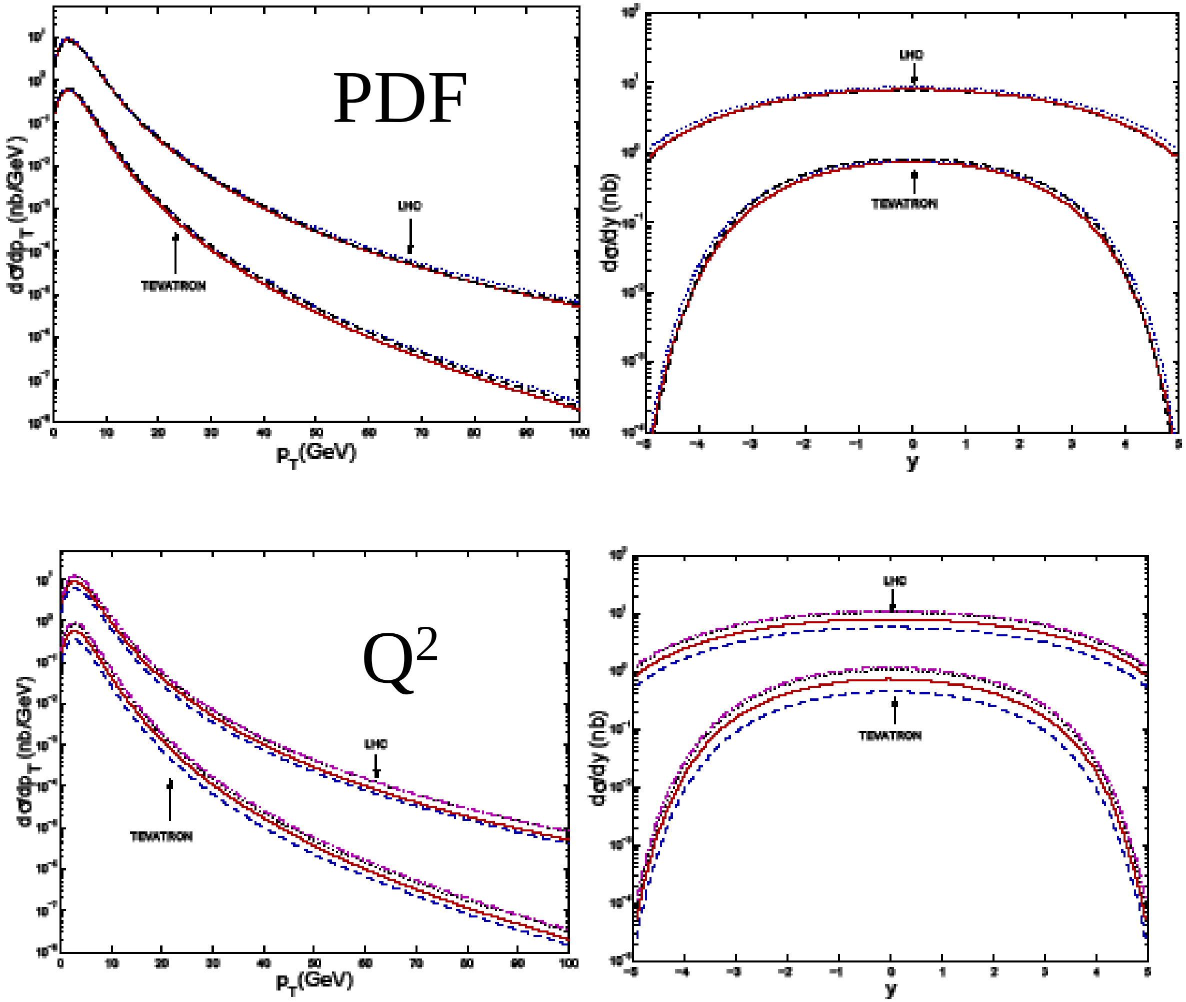

Uncertainties

α_s

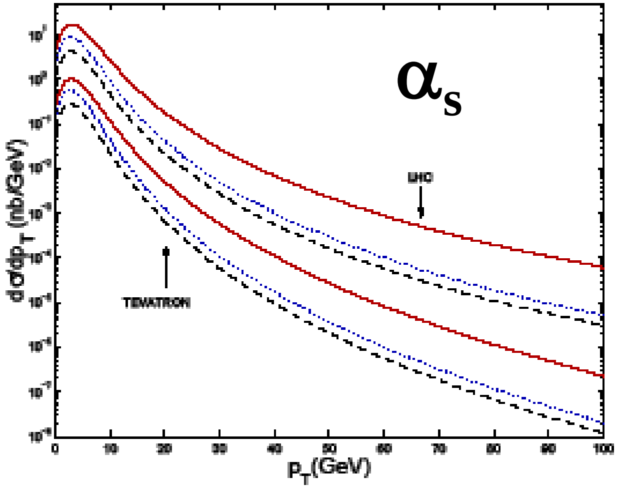

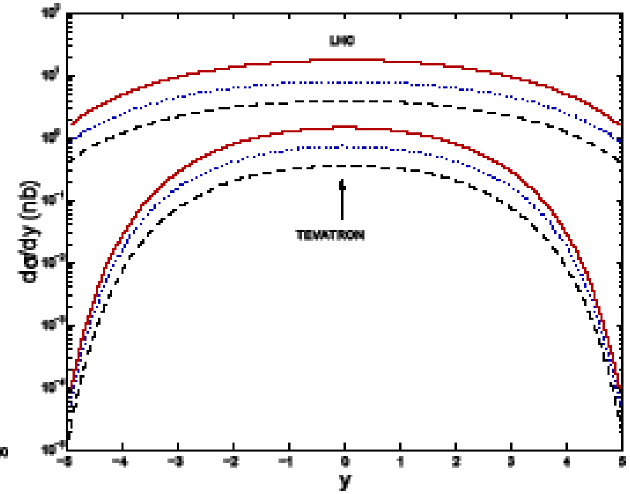

Mechanism

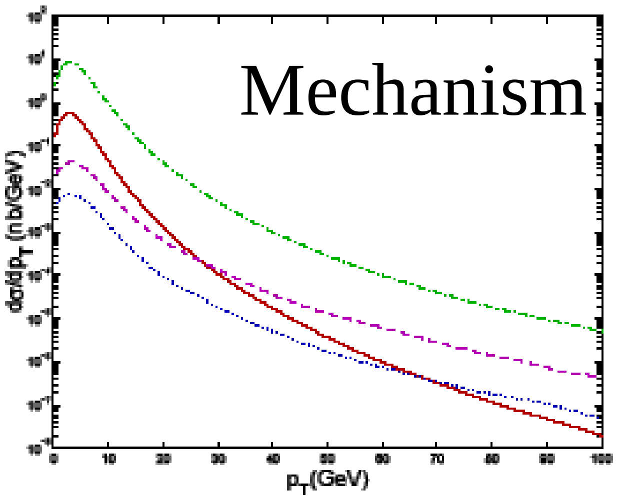

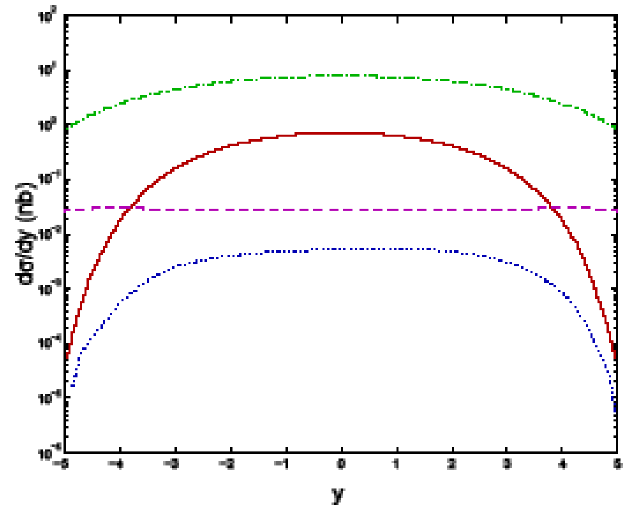

Cross-section

TABLE III: Total cross-section for the hadronic production of $B_c[1^1S_0]$ and $B_c^*[1^3S_1]$ at TEVATRON and at LHC with the leading order (LLO) running α_s and the characteristic energy scale $Q^2 = \hat{s}/4$ or $Q^2 = p_T^2 + m_{B_c}^2$. The cross section is in unit of nb.

	CTEQ5L	CTEQ6L	GRV98L	MRST2001L	CTEQ5L	CTEQ6L	GRV98L	MRST2001L
-	$Q^2 = \hat{s}/4$				$Q^2 = p_T^2 + m_{B_c}^2$			
-	TEVATRON							
$\sigma_{B_c(1^1S_0)}$	3.12	3.79	3.27	3.40	4.39	5.50	4.54	4.86
$\sigma_{B_c^*(1^3S_1)}$	7.39	9.07	7.88	8.16	10.7	13.4	11.1	11.9
-	LHC							
$\sigma_{B_c(1^1S_0)}$	49.8	53.1	53.9	47.5	65.3	71.1	70.0	61.4
$\sigma_{B_c^*(1^3S_1)}$	121.	130.	131.	116.	164.	177.	172.	153.

TABLE VI: The integrated hadronic cross section for TEVATRON at different C.M. energies. The gluon distribution is chosen from CTEQ5L and the characteristic energy scale of the production is chosen as Type A, i.e. $Q^2 = \hat{s}/4$. In addition, a cut for transverse momentum p_T ($p_T < 5$ GeV) and a cut for rapidity y ($|y| > 1.5$) have been imposed.

20%

C.M. energy	1.8(TeV)	1.9(TeV)	1.96(TeV)	2.0(TeV)
$B_c[^1S_0]$	0.40	0.44	0.46	0.47
$B_c^*[^3S_1]$	1.00	1.09	1.14	1.18

P_T cut

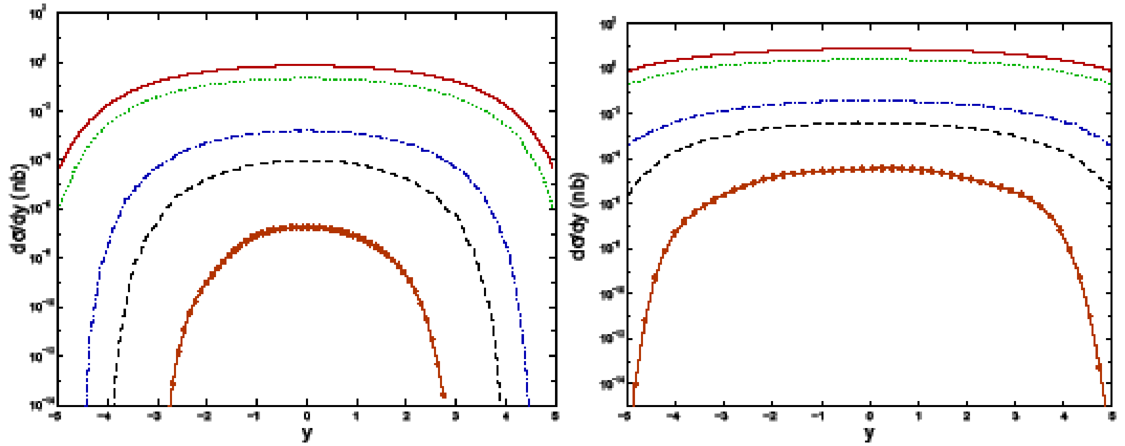

FIG. 6: B_c differential distributions versus its y with various p_{Tcut} in TEVATRON (left diagram) and in LHC (right diagram). Solid line corresponds to the full production without p_{Tcut}; dashed line to $p_{Tcut} = 5.0$ GeV; dash-dot line to $p_{Tcut} = 20.0$ GeV; the dashed line to $p_{Tcut} = 35.0$ GeV; the big dotted line to $P_{Tcut} = 50.0$ GeV and the solid line with diamonds to $p_{Tcut} = 100$ GeV.

TABLE V: Values of the ratio $R_{p_{Tcut}}$ (see definition in text) for the hadronic production of pseudo-scalar B_c meson in TEVATRON and LHC.

p_{Tcut}	0.0 GeV			5 GeV			20 GeV			35 GeV			50 GeV		
y_{cut}	1.0	1.5	2.0	1.0	1.5	2.0	1.0	1.5	2.0	1.0	1.5	2.0	1.0	1.5	2.0
$R_{p_{Tcut}}$ (TEVATRON)	0.45	0.64	0.79	0.46	0.65	0.80	0.57	0.77	0.91	0.65	0.85	0.95	0.70	0.90	0.98
$R_{p_{Tcut}}$ (LHC)	0.31	0.46	0.59	0.32	0.47	0.60	0.38	0.54	0.69	0.42	0.60	0.74	0.45	0.64	0.79

Results for the P-wave Bc states

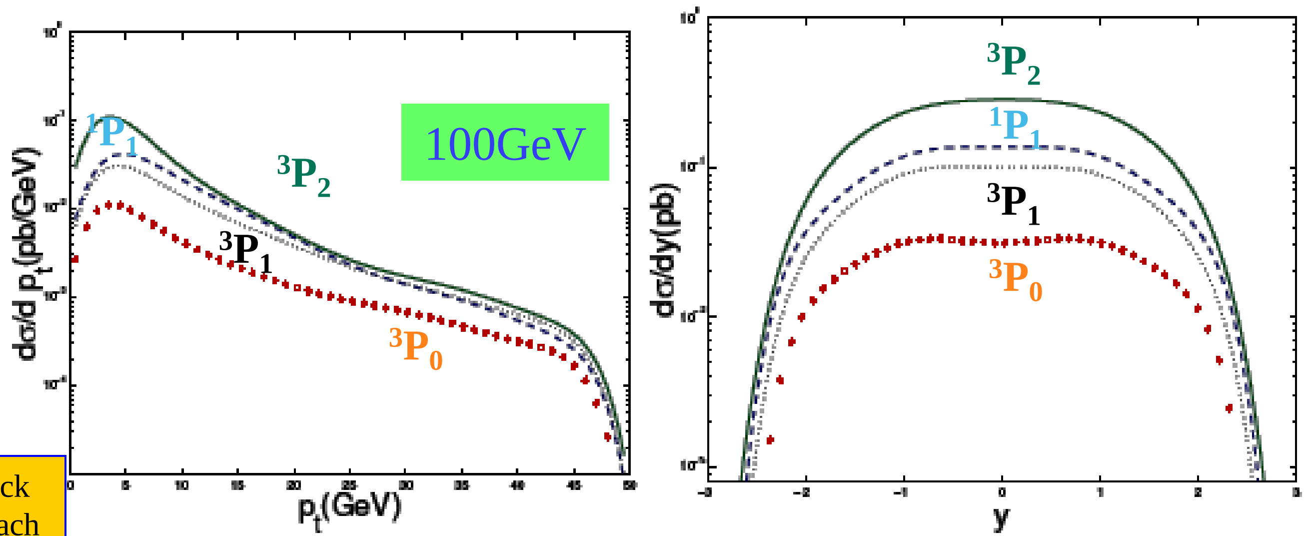

subprocess

Good check between each other !!!

C.M. energy (GeV)	20GeV	40GeV	60GeV	80GeV	100GeV	200GeV
$\sigma(^1P_1)(pb)$	0.184	0.743	0.657	0.538	0.439	0.195
$\sigma(^3P_0)(pb)$	0.367	0.207	0.175	0.141	0.114	0.0496
$\sigma(^3P_1)(pb)$	0.346	0.598	0.503	0.402	0.324	0.139
$\sigma(^3P_2)(pb)$	0.721	1.49	1.31	1.06	0.862	0.374

A.V. Berezhnoy,

totally numerically

total hadronic production

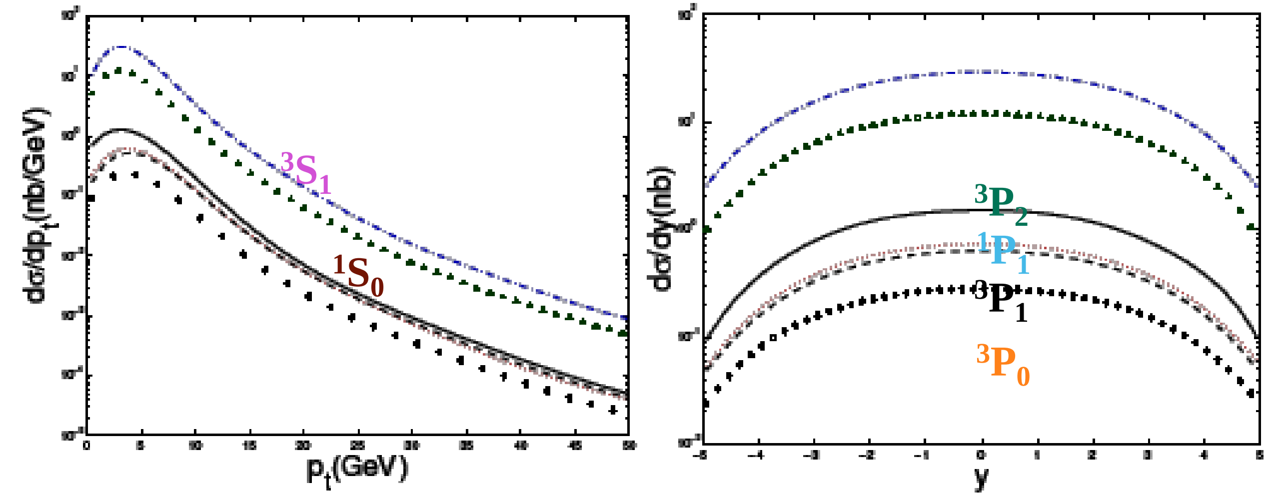

LHC

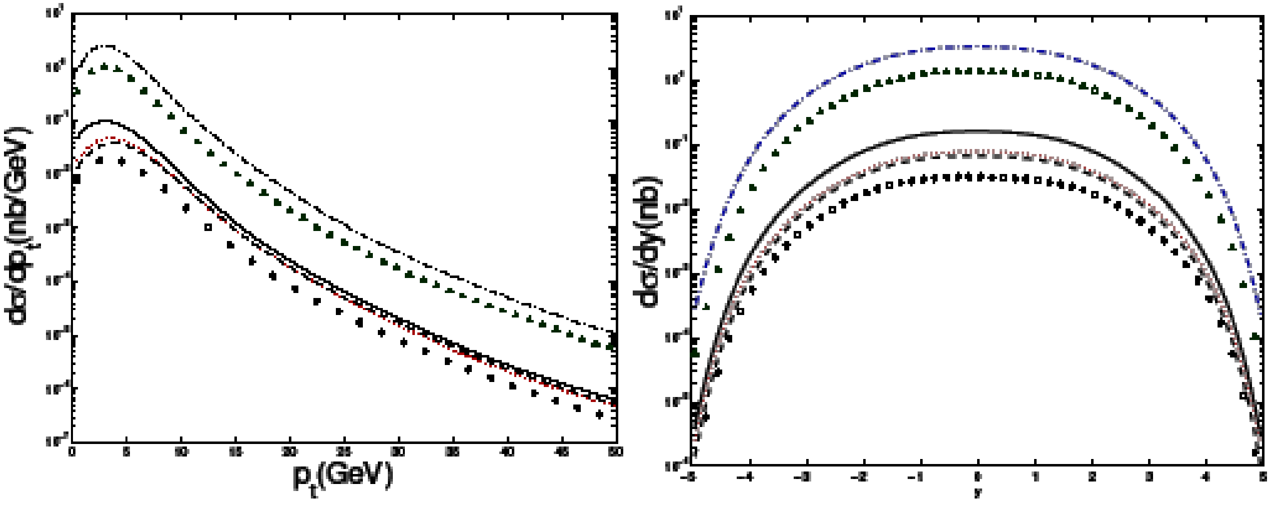

TEVATRON

Cross-section

-	LHC ($\sqrt{S}=14.$ TeV)				TEVATRON ($\sqrt{S}=1.96$ TeV)			
Q^2	A	B	C	D	A	B	C	D
$\sigma(^1P_1)(nb)$	4.738	9.123	9.825	8.379	0.2555	0.6545	0.7547	0.5507
$\sigma(^3P_0)(nb)$	1.910	3.288	3.523	3.036	0.1161	0.2563	0.2966	0.2149
$\sigma(^3P_1)(nb)$	4.117	7.382	7.304	6.682	0.2289	0.5597	0.6490	0.4780
$\sigma(^3P_2)(nb)$	10.18	20.40	21.71	18.26	0.5096	1.350	1.515	1.102

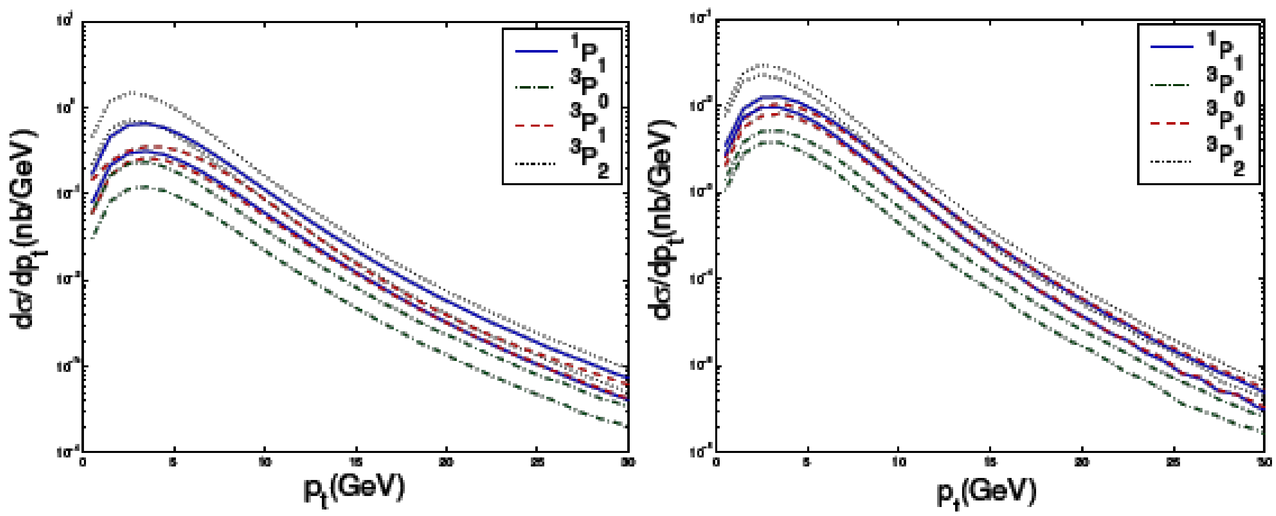

A.V. Berezhnoy,

LHC

TEVATRON

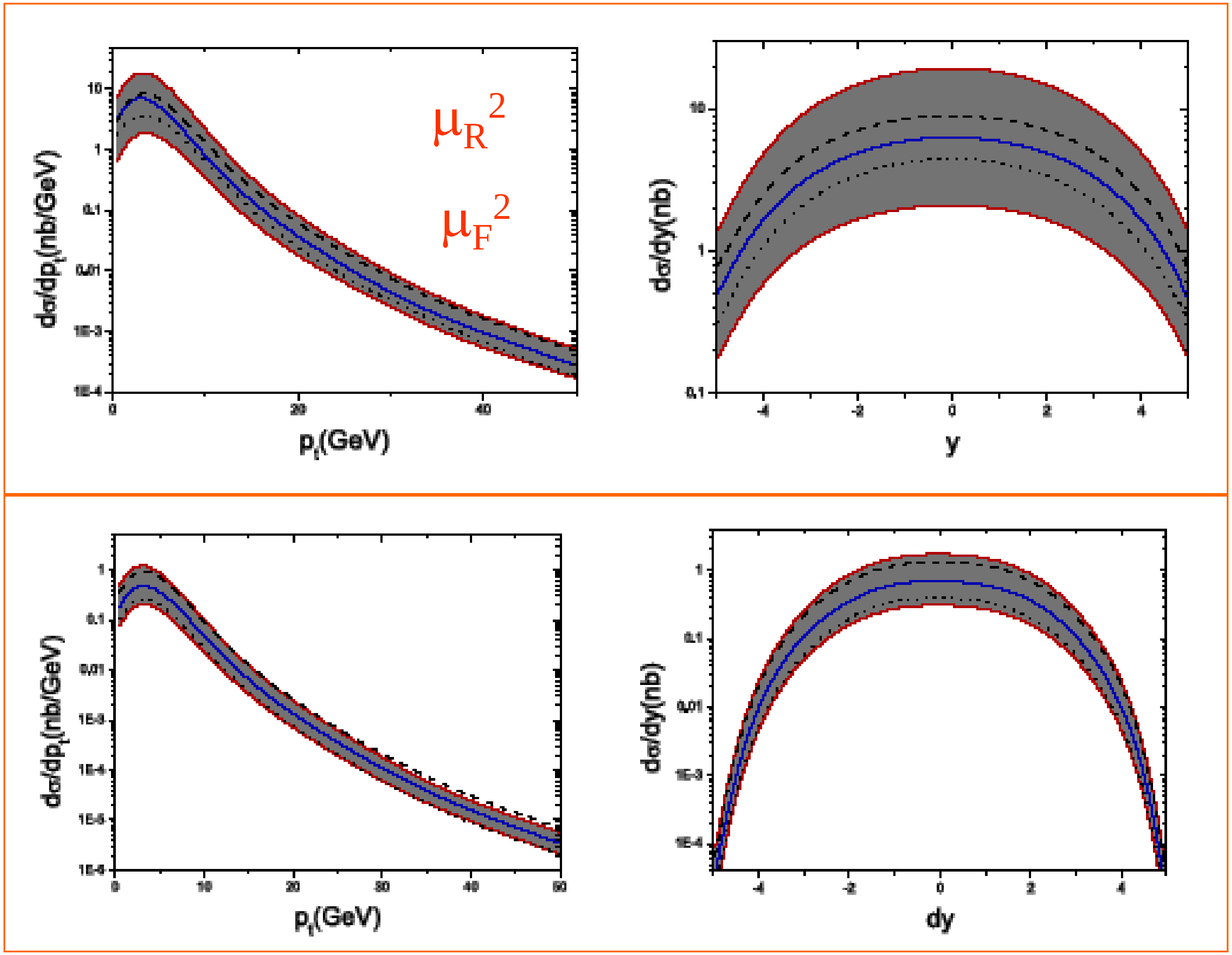

For experimental usage

y cut

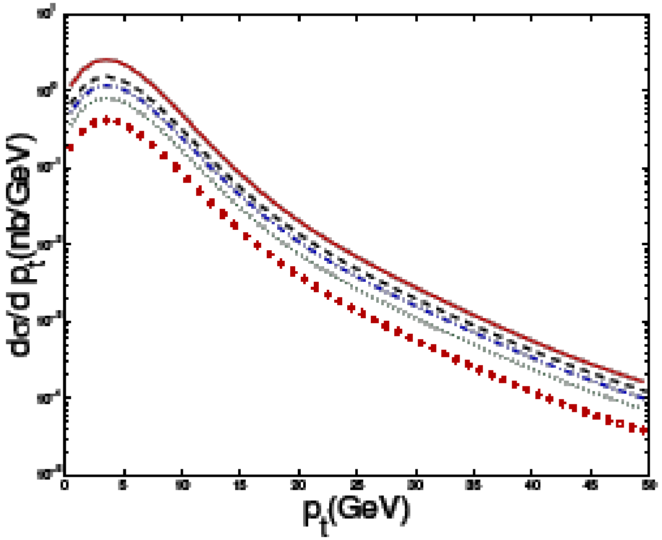

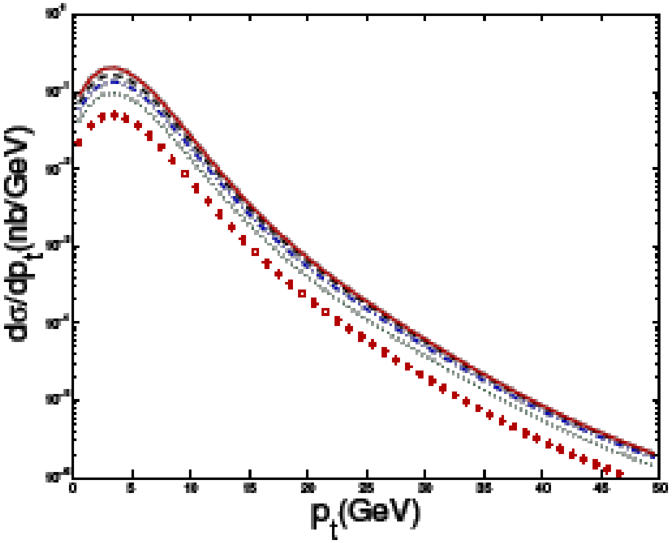

P_T cut

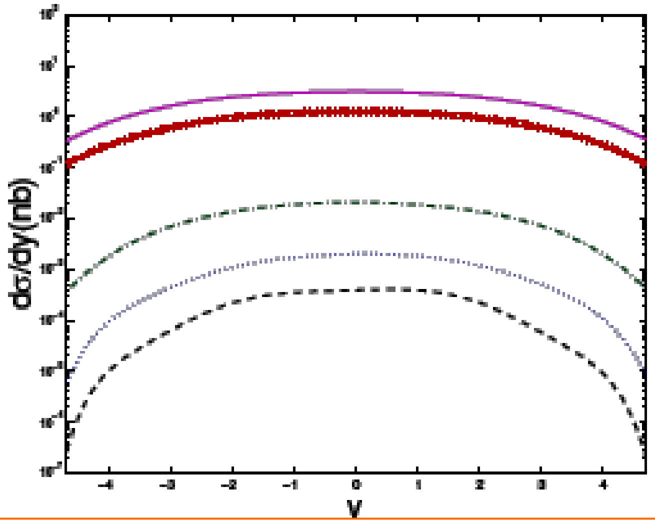

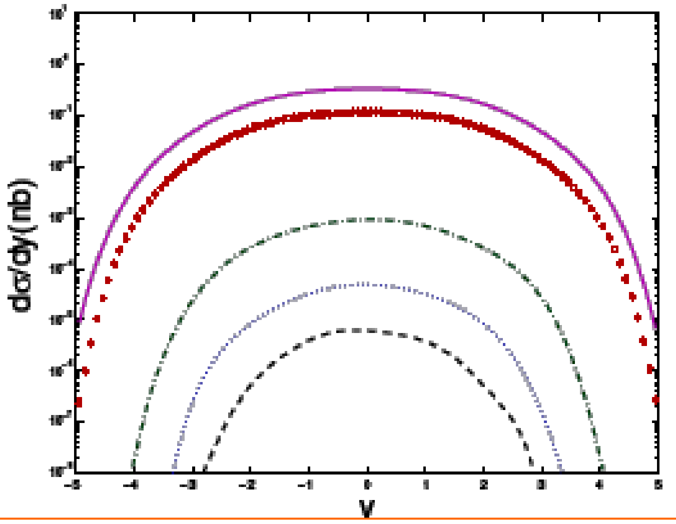

Results for the color-octet Bc states

TABLE I: Total cross-section (in unit of nb) for the hadronic production of the $(c\bar{b})$ meson at LHC (14.0 TeV) and TEVATRON (1.96 TeV), where for short the $|(^1S_0)_1\rangle$ denotes $(c\bar{b})$ state in color-singlet $(^1S_0)$ configuration, and so forth. Here $m_b = 4.90$ GeV, $m_c = 1.50$ GeV and $M = 6.40$ GeV. For the color-octet matrix elements, we take $\Delta_S(v) \in (0.10,\ 0.30)$.

-	$\|(^1S_0)_1\rangle$	$\|(^3S_1)_1\rangle$	$\|(^1S_0)_8 g\rangle$	$\|(^3S_1)_8 g\rangle$	$\|(^1P_1)_1\rangle$	$\|(^3P_0)_1\rangle$	$\|(^3P_1)_1\rangle$	$\|(^3P_2)_1\rangle$
LHC	71.1	177.	(0.357, 3.21)	(1.58, 14.2)	9.12	3.29	7.38	20.4
TEVATRON	5.50	13.4	(0.0284, 0.256)	(0.129, 1.16)	0.655	0.256	0.560	1.35

-	$\|(^1S_0)_1\rangle$	$\|(^3S_1)_1\rangle$	$\|(^1S_0)_8 g\rangle$	$\|(^3S_1)_8 g\rangle$	$\|(^1P_1)_1\rangle$	$\|(^3P_0)_1\rangle$	$\|(^3P_1)_1\rangle$	$\|(^3P_2)_1\rangle$
LHC	1.00	2.48	(0.005, 0.045)	(0.022, 0.199)	0.128	0.046	0.103	0.287
TEVATRON	1.00	2.44	(0.005, 0.046)	(0.023, 0.211)	0.119	0.046	0.102	0.245

3-20%

60%

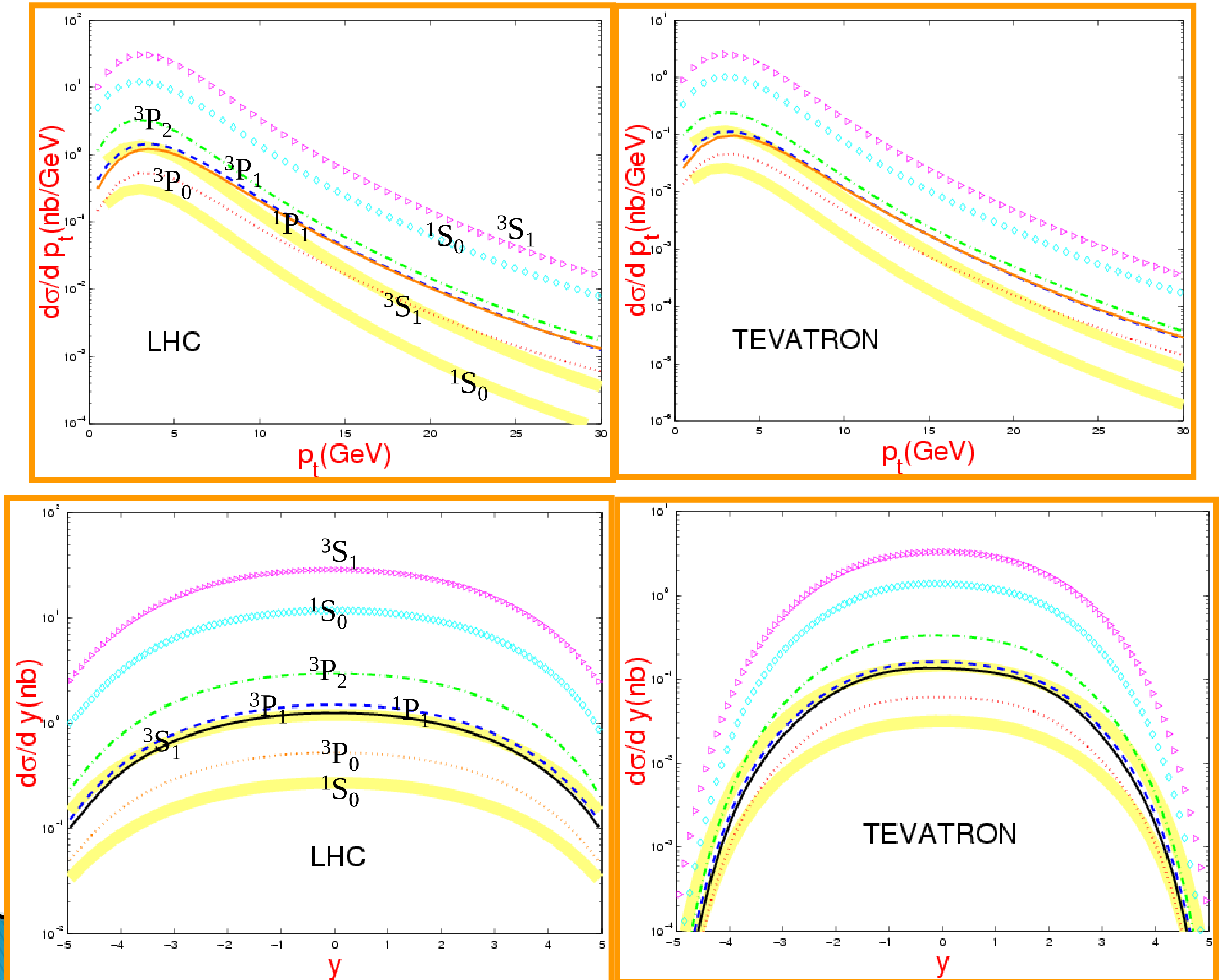
LHC
TEVATRON
LHC
TEVATRON
dσ/d p_t (nb/GeV)
p_t (GeV)
dσ/d y (nb)
y
³S₁
¹S₀
³P₂
³P₁
¹P₁
³P₀

Results for Xicc, Xibc and Xibb Production

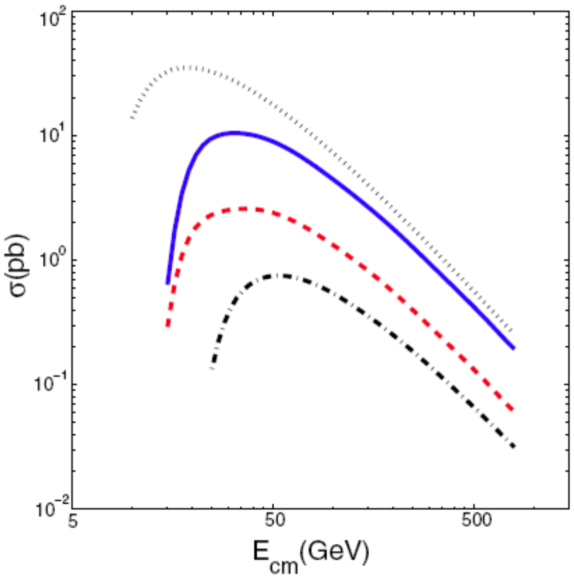

FIG. 5 (color online). The energy dependence of the integrated partonic cross-section for the production of the baryons via the heavy diquarks in terms of the gluon-gluon fusion mechanism. The dotted line, solid line, dashed line and dash-dot line stand for those via the diquarks $(cc)_{\bar{3}}[^3S_1]$, $(bc)_{\bar{3}}[^3S_1]$, $(bc)_{\bar{3}}[^1S_0]$ and $(bb)_{\bar{3}}[^3S_1]$ respectively. The curves for Ξ_{cc} and Ξ_{bb} both are divided by 2.

TABLE II. Cross sections (σ) for the hadronic production of Ξ_{cc} at colliders TEVATRON and LHC, where the (cc)-diquark is in $(cc)_{\bar{3}}[^3S_1]$ or $(cc)_6[^1S_0]$, and the symbol $g + c$ means $g + c \to \Xi_{cc} + \bar{c}$ and etc. In the calculations, cuts $p_t \geq 4$ GeV and $|y| \leq 1.5$ are taken at LHC, while at TEVATRON cuts $p_t \geq 4$ GeV, $|y| \leq 0.6$ instead.

–	TEVATRON ($\sqrt{S} = 1.96$ TeV)		LHC ($\sqrt{S} = 14.0$ TeV)	
–	$(cc)_{\bar{3}}[^3S_1]$	$(cc)_6[^1S_0]$	$(cc)_{\bar{3}}[^3S_1]$	$(cc)_6[^1S_0]$
$\sigma_{g+g}(nb)$	1.61	0.392	22.3	5.44
$\sigma_{c+g}(nb)$	2.29	0.360	22.1	3.42
$\sigma_{c+c}(nb)$	0.751	0.0431	8.74	0.475

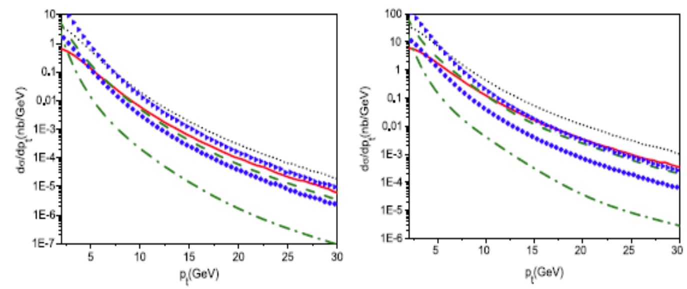

FIG. 9 (color online). The p_t-distribution for the hadroproduction of Ξ_{cc} at TEVATRON (left) and at LHC (right), where $|y| \leq 1.5$ at LHC and $|y| \leq 0.6$ at TEVATRON are adopted. The dotted line and the solid line are for gluon-gluon fusion mechanism, the triangle line and the diamond line are for $g + c \to \Xi_{cc} + \bar{c}$, the dashed line and the dash-dot line are for $c + c \to \Xi_{cc} + `g'$, where the upper lines of each mechanism are for $(cc)_{\bar{3}}[^3S_1]$ and the lower lines are for $(cc)_6[^1S_0]$, respectively.

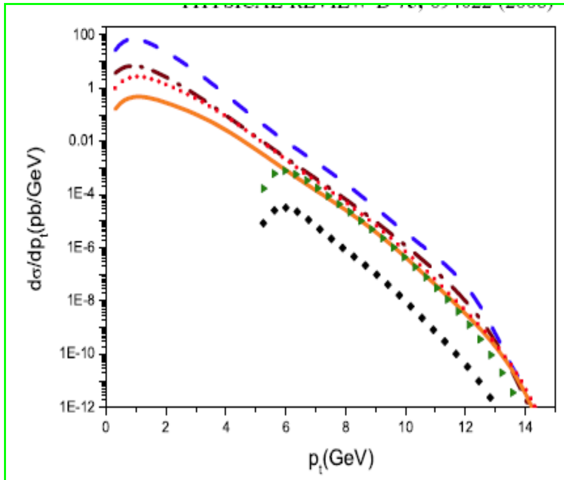

FIG. 10 (color online). The p_t-distributions for the hadroproduction of Ξ_{cc} at SELEX. The dotted line and the solid line are for gluon-gluon fusion mechanism, the dashed line and the dash-dot line are for $g + c \to \Xi_{cc} + \bar{c}$, the triangle line and the diamond line are for $c + c \to \Xi_{cc} + {}'g'$, where the upper lines of each mechanism are for $(cc)_{\bar{3}}[^3S_1]$ and the lower lines are for $(cc)_6[^1S_0]$, respectively.

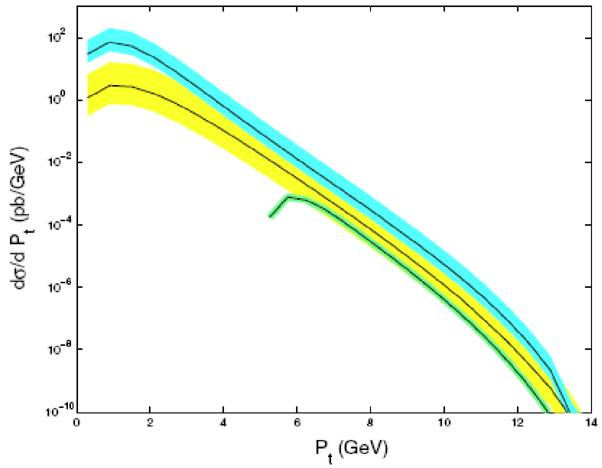

FIG. 11 (color online). The energy scale dependence of the p_t-distributions for each mechanism at SELEX, where the contributions from $(cc)_{\bar{3}}[^3S_1]$ and $(cc)_6[^1S_0]$ are summed up. The upper band is for the mechanism $g + c \to \Xi_{cc}$, the middle band is for gluon-gluon fusion mechanism and the lower band is for $c + c \to \Xi_{cc}$ mechanism, where the solid line in each band corresponds to $\mu = M_t$, the upper edge of the band is for $\mu = M_t/2$ and the lower edge is for $\mu = 2M_t$, respectively.

$$R = \frac{\sigma_{\text{total}}}{\sigma_{gg \to \Xi_{cc}((cc)_{\bar{3}}[^3S_1])}},$$

TABLE IV. R values, which is defined in Eq. (10), for the hadronic production of Ξ_{cc}.

	SELEX	TEVATRON	LHC
-	$p_t > 0.2$ GeV	$p_t \geq 4$ GeV, $\lvert y\rvert \leq 0.6$	$p_t \geq 4$ GeV, $\lvert y\rvert \leq 1.5$
R	29	3.4	2.8

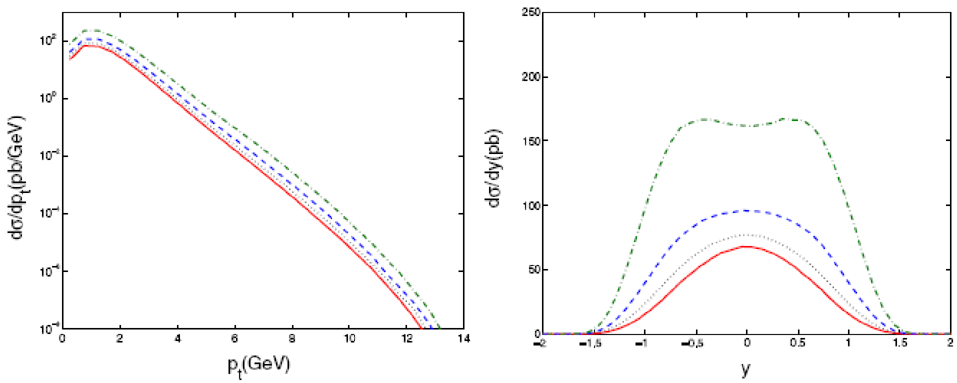

Figure 3. The p_t-distributions (left) and y-distributions (right) for the hadroproduction of Ξ_{cc} at SELEX with different values of $A_{\rm in}$. The dotted, the dashed and the dash-dotted lines are for $A_{\rm in} = 0.1\%, 0.3\%$ and 1%, respectively. The result with CTEQ6HQ, i.e., $A_{\rm in} = 0$ is shown by a solid line (the lowest one).

Table 1. The contribution of σ_{ab} from different sub-processes initialized by the partons ab to the total cross section (in pb) for the Ξ_{cc} hadronic production at SELEX with the cut $p_t > 0.2$ GeV.

	CTEQ6HQ($A_{\rm in} = 0$)			$A_{\rm in} = 1\%$		
	σ_{gg}	σ_{cc}	σ_{gc}	σ_{gg}	σ_{cc}	σ_{gc}
$(cc)_{\bar{3}}[^3S_1]$	4.03	1.02×10^{-3}	102.	4.06	1.25×10^{-2}	372
$(cc)_6[^1S_0]$	0.754	4.15×10^{-5}	11.3	0.758	5.01×10^{-4}	40.9

Table 2. The contribution rates of the sub-process $gc \to \Xi_{cc}$ in the different x region in the charm quark PDFs with $A_{in} = 1\%$ and $p_t > 0.2$ GeV.

$0.0 \leqslant x_c \leqslant 0.2$	$0.2 \leqslant x_c \leqslant 0.4$	$0.4 \leqslant x_c \leqslant 0.6$	$0.6 \leqslant x_c \leqslant 0.8$	$0.8 \leqslant x_c \leqslant 1.0$
25%	50%	22%	3%	~0

Table 3. The R values for SELEX with the cut $p_t > 0.2$ GeV.

	CTEQ6HQ ($A_{\rm in} = 0$)	$A_{\rm in} = 0.1\%$	$A_{\rm in} = 0.3\%$	$A_{\rm in} = 1\%$
R	29.3	36.6	51.3	103.

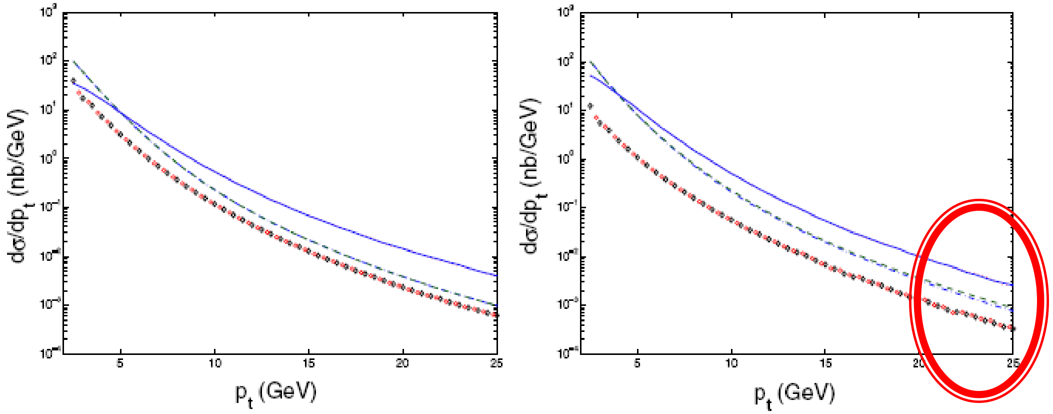

Figure 5. The p_t-distributions for the hadroproduction of Ξ_{cc} at LHC. The left figure is for CMS or ATLAS with the rapidity cut $|y| \leqslant 1.5$ being adopted and the right one is for LHCb with the pseudo-rapidity cut $1.8 \leqslant |\eta| \leqslant 5.0$ being adopted. The solid line, the dash-dotted line and the circle line correspond to that of the $g+g$, $g+c$ and $c+c$ mechanisms without the intrinsic charm being considered (the PDFs in CTEQ6HQ [8] are used), respectively. The dotted line, the dashed line and the diamond line correspond to that of the $g+g$, $g+c$ and $c+c$ mechanisms with the intrinsic charm being considered (the PDFs of equation (6) with $A_{\rm in} = 1\%$ are used), respectively. The differences with and without intrinsic charm are so small that, of them, only at LHCb for the $g+c$ mechanism the difference can be seen from the right figure.

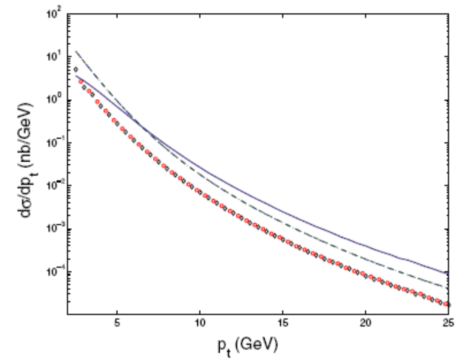

Figure 6. The p_t-distributions for the hadroproduction of Ξ_{cc} at TEVATRON with the rapidity cut $|y| \leqslant 0.6$ being adopted. The meaning for the lines in the figure is the same as figure 5. The differences between the two cases with and without intrinsic charm are too small to be seen.

LHC, TEVATRON can not see the difference between the cases of with or with intrinsic charm

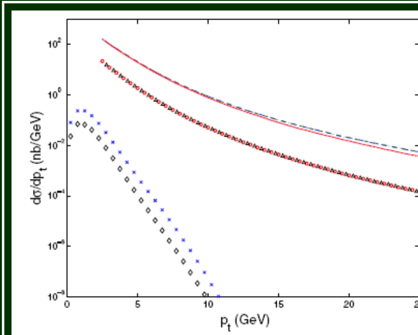

Figure 8. The p_t-distributions for the hadroproduction of Ξ_{cc}. The dotted line, the dash-dotted line, the circle line and the diamond line are those corresponding to LHCb, LHC, Tevatron and SELEX with $A_{\rm in} = 0$, respectively. The solid, the dashed line, the triangle line and the cross line are those corresponding to LHCb, LHC, Tevatron and SELEX with $A_{\rm in} = 1\%$, respectively. Only at SELEX, the difference between the cases with and without intrinsic charm can be seen.